2023-08-01

# Structural Study Of LSD13 And LSD14 Type I Modular Polyketide Synthases From The Lasalocid A Biosynthesis Pathway

Dayan Viera
*University of Texas at El Paso*

# STRUCTURAL STUDY OF LSD13 AND LSD14 TYPE I MODULAR POLYKETIDE SYNTHASES FROM THE LASALOCID A BIOSYNTHESIS PATHWAY

DAYAN VIERA

Master's Program in Chemistry

APPROVED:

Chu-Young Kim, Ph.D., Chair

Mahesh Narayan, Ph.D.

Lela Vukovic, Ph.D.

Irimpan Mathews, Ph.D.

Stephen L. Crites, Jr., Ph.D.
Dean of the Graduate School

# STRUCTURAL STUDY OF LSD13 AND LSD14 TYPE I MODULAR POLYKETIDE SYNTHASES FROM THE LASALOCID A BIOSYNTHESIS PATHWAY

by

B.S. DAYAN VIERA

THESIS

Presented to the Faculty of the Graduate School of

The University of Texas at El Paso

in Partial Fulfillment

of the Requirements

for the Degree of

MASTER OF SCIENCE

Department of Chemistry and Biochemistry

THE UNIVERSITY OF TEXAS AT EL PASO, TX

August 2023

## Abstract

Bioactive natural products often possess a complex structure and have a large size which make their chemical synthesis highly challenging. To overcome this challenge, we are developing a biosynthetic method for production of natural products and their analogs. This technology is expected to decrease the synthesis time from years to weeks and reduce the cost of drug production by multiple orders of magnitude. We are investigating the biosynthesis pathway of lasalocid A, an anticancer antibiotic, to develop this technology. Specifically, we aim to characterize the enzymes structurally and biochemically in this pathway, thus paving the way for their rational engineering. We have expressed and purified the recombinant Lsd13 and Lsd14 polyketide synthases, two key enzymes from the lasalocid A biosynthesis pathway. We have also obtained potential crystals of the Lsd13 protein and potential crystals of the partial Lsd13-Lsd14 complex. We will use these crystals to perform X-ray diffraction experiments in the future and ultimately determine their atomic structure. We have also characterized the binding interaction between Lsd13 and Lsd14 using surface plasmon resonance spectroscopy. Our results suggest that Lsd13 and Lsd14 are dimeric proteins and that they form a stable complex to allow transfer of the intermediate polyketide chain product from Lsd13 to Lsd14.

**Acknowledgement**

I would like to extend my sincere gratitude towards my project supervisor Dr. Chu-Young Kim. Thank you, Dr. Kim, for accepting me in your research group and giving me an opportunity to grow as a person and student. I would also like to thank members of the lab including Dr. Priyanka Gade, Afroz Karim, Haram Cha, Dr. Anwar Ullah, Dr. Manas Jagdev, Gerardo Vargas and **Gileydis Guillama** for providing me with useful suggestions.

Thanks to my family for their constant support throughout this journey, and especially my grandfather, I know he would love to see me achieve my goals.

Thank you to my wife for the constant support these years even in the lab, just THANK YOU.

## Table of Contents

## List of Figures

# Introduction

The emergence of drugs resistance is a significant hurdle in modern medicine, driven by the evolutionary pressure for survival. This resistance poses a major challenge as it compromises the effectiveness and longevity of drugs, limiting treatment options for patients, with high prevalence in all areas of oncology and infectious diseases. Any biological entity capable of creating diversity and evolving can develop resistance(Kurt Yilmaz & Schiffer, 2021). Pathogens including bacteria, viruses and fungi undergo evolutionary changes to withstand the effects of antimicrobials, which include antibiotics, antivirals and antifungals (W. Wang et al., 2018).

Due the constant increasing of this resistance a variety of techniques across scientific fields, including structural biology, medicinal chemistry, enzymology, computational chemistry, nanotechnology, systems biology, and ethnobotany, are applied to identify the mechanisms behind drug resistance and explore potential novel drug candidates. Over the last century, pharmaceutical industry-developed drugs have profoundly transformed medical practices and influenced various facets of our culture, primarily through a target-agnostic and mechanism-agnostic approach to drug discovery. The development in organic chemistry leading to combinatorial synthesis (Kennedy et al., 2008) and the implementation with high throughput (Liu et al., 2017) techniques revolutionized the field increasing the automatization and speed to generate huge compounds libraries.

The process of drug discovery is characterized by its high cost, extensive time requirements and the absence of a guarantee in developing a novel drug for disease treatment. Reassuringly, the number of new FDA-approved drugs has been increasing, and the current 5-year annual approval rate average is double what it was in 2009 (Darrow et al., 2020). Being the organic synthesis the

more challenging step due to the difficulties on the synthesis of usually very complex molecules or even the modification of very complex drug structures. Numerous reviews have described the importance of compounds derived from microorganism, plant and animal sources to treat human diseases (Gershell & Atkins, 2003; Lam, 2007).

### 1.1. Polyketide natural products

Polyketides are secondary metabolites of bacteria, fungi, plants, and animals. Polyketides are biosynthesized by the polymerization of acetyl, and propionyl subunits obtained by decarboxylation of malonyl coenzyme A in a process like fatty acid biosynthesis. Contain multiple β-hydroxyketone or β-hydroxy aldehyde functional groups, which are further modified into bioactive natural products with diverse biological activities and pharmacological properties (Ridley et al., 2008; Robinson, 1991).

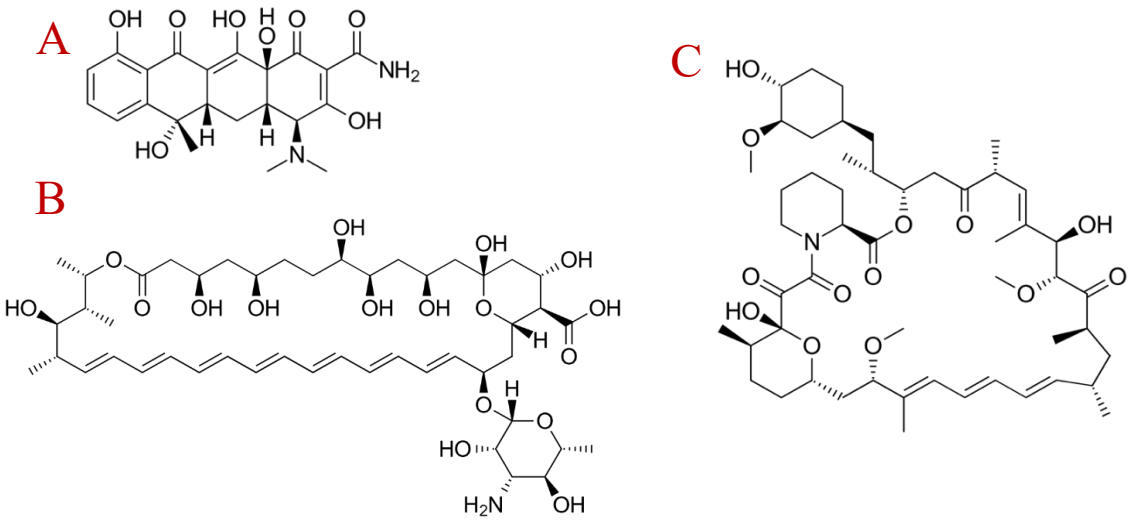


***Figure 1.*** *Structures of tetracycline (A), amphotericin (B) and rapamycin (C)*

Polyketides exhibit a wide range of bioactivities such as antibacterial (e.g., tetracycline), anti-cholesterol (e.g., lovastatin), anticancer (e.g., doxorubicin), antifungal (e.g., amphotericin B),

antiviral (e.g., balticolid), immune suppressing (e.g., rapamycin) and anti-inflammatory activity (e.g., flavonoids). **(Figure 1)**

### 1.2. Polyketides Biosynthesis

The polyketide biosynthesis mechanism is in fact a biological factory where each module and domain functions as part of an assembly line. The synthesis (elongation) of the polyketide chain, begins with the loading of the initial unit in the LDD module and ends with the desired structure being released by the TE module. A typical elongation step, that takes place in a single module, starts when the Acyltransferase (AT) selects the appropriate extender unit to be incorporated in the growing polyketide chain. Acyl carrier protein (ACP) serves as a covalent attachment point for the intermediate during the assembly process. The intermediate is attached to the phosphopantetheine (Ppant) prosthetic group present on the ACP. The Ketosynthase (KS) domain then joins the building block chosen by AT to the growing polyketide chain using Claisen- condensation reaction(Weissman, 2009). On the other hand, Ketoreductase (KR), dehydratase (DH) and enoyl reductase (ER) are non-condensing domains that do not affect the length of the polyketide chain. These domains will reduce the β-keto group respectively to an hydroxyl, α,β-double bond, or fully reduced methylene. Thioesterase domain (TE) catalyzes the cyclization α,β-double bond methylene group and facilitates the release of the polyketide chain from the polyketide synthase (Risdian et al., 2019).

### 1.3. Polyketides synthases enzymes (PKS)

Polyketides are a family of multi-functional enzymes or enzymes complexes that produces polyketides. The polyketides synthases are categorized in three categories, Type I, Type II and

Type III(Weissman, 2009). The type I polyketide synthases involve huge multifunctional proteins that have many modules containing some domains, in which a particular enzymatic reaction occurs. A domain is a defined region of a protein or enzyme that have a particular function or make a particular transformation over the substrate molecule(Katz, 1997).Type I PKSs are generally responsible for producing macrocyclic polyketides. Each module has the responsibility of performing one condensation cycle in a non-iterative way (Li et al., 2010; B. Wang et al., 2020). These domains are grouped into modules, like the *Elongation or extending modules and termination* or *releasing module* (-TE).

The Type II polyketide synthases (type II PKSs) are iterative and consist of discrete catalytically functional enzymes which associate and form complexes to produce the polyketide product upon iterations through a defined number of chain extension cycles (Shen, 2003).

In contrast to type I and type II PKSs, the type III PKSs operate without utilizing ACP as a tether to produce polyketide metabolite, also, employing acyl-CoAs directly as substrates (Shen, 2003).

### 1.4. Lasalocid and its biosynthesis pathway

Lasalocid A **(Figure 2)** is an antibacterial agent which is produced by the strains of *Streptomyces lasaliensis*. It is of commercial value and is one of the active components in the feed additives called Bovatec(Dzikamunhenga & Griffith, 2012). It is a polyether ionophore and hence can induce ion transport across a polar phase (including lipid bilayer membranes) by forming complexes with monovalent and divalent cations, it can also transport big organic cations like dopamine.(Duax et al., 1996)

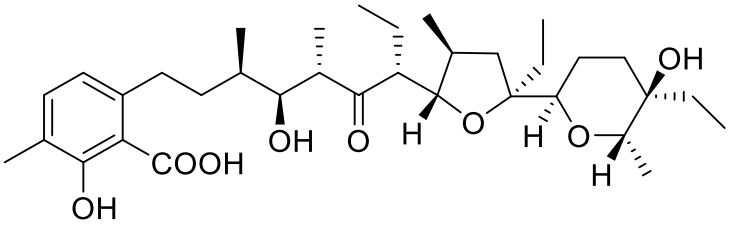


***Figure 2.*** *Lasalocid A structure.*

The total synthesis of this compound is really challenging, and even though as today there are several reports and methodologies, as the first total synthesis reported by Y. Kishi in 1978(Nakata et al., 1978), with a 16 steps mechanism; and others reports like Stereoselective C-O Ring Construction: The Oguri-Oikawa Synthesis of Lasalocid A reported by Douglass F. Taber, 2011 with more than 25 synthesis steps scheme and with an overall yield less than 10%(Taber, 2011). Recently, the Streptomyces lasaliensis gene cluster for lasalocid A biosynthesis has been elucidated, consists of 7 type I polyketide synthases containing one loading module and 11 extension modules (Lsd11- Lsd17), an epoxidase (Lsd18) and an epoxide hydrolase (Lsd19) **(Figure 3)**(Migita et al., 2009). This biosynthetic pathway is expected to produce a linear 12-carbon polyketide chain adding up five malonyl-CoA, four methyl malonyl-CoA and three ethyl malonyl-CoA subunits that subsequently undergoes aromatization to form the 3-methylsalicylate head group, giving rise to prelasalocid A. Following that, the epoxidase enzyme Lsd18 transform the two E-olefins into epoxides, resulting in the formation of bisepoxyprelasalocid A. Finally, an epoxide hydrolase, catalyzes two consecutive epoxide-opening cyclization reactions, one exo-cyclization and one anti-Baldwin-type endo cyclization, on bisepoxyprelasalocid A to give the final product Lasalocid A (Zhang et al., 2017).

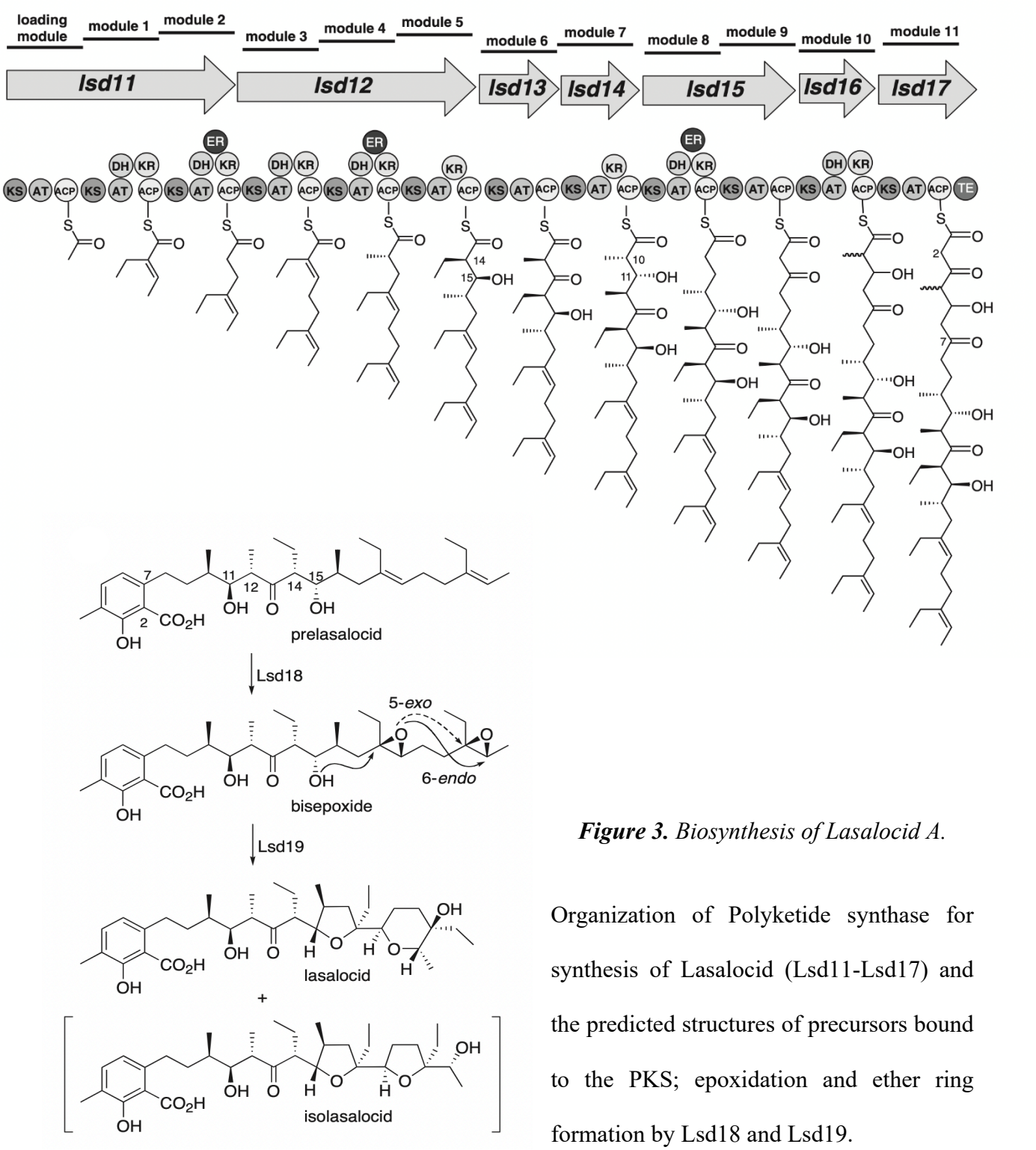


***Figure 3.*** *Biosynthesis of Lasalocid A.*

Organization of Polyketide synthase for synthesis of Lasalocid (Lsd11-Lsd17) and the predicted structures of precursors bound to the PKS; epoxidation and ether ring formation by Lsd18 and Lsd19.

Lsd11 Lsd12 contains three modules including the loading module in Lsd11, Lsd15 contain two modules and Lsd13, Lsd14, Lsd16 and Lsd17 contain one module each. Hence this system provides opportunities to study interactions between modules, which are part of separate polypeptides and single polypeptide chain. NMR and X-ray structures for individual domains of other polyketide synthases have been solved (Moretto et al., 2019; L. Wang et al., 2019).

### 1.5. Lsd14 polyketide synthase

To date there is only one high-resolution structure of a type I modular PKS from this pathway, Lsd14(Bagde et al., 2021). All Lsd synthases proteins involved in Lasalocid A biosynthesis are dimers, in this case Lsd14 has a compact homodimer structure, with the dimer interface formed by N-terminal Docking domains (DD/DD′) (~524 Å), KS/KS′ (~1952 Å), and pre-KR dimerization element (DE), DE/DE′ (~826 Å). The two Acyltransferase (AT) domains are positioned at opposite ends of the Ketosynthase (KS) dimer and are linked to the KS domain through a well-structured linker domain (LD). The $(KS\text{-}LD\text{-}AT)_2$ dimer, denoted as KS-LD-AT/KS′-LD′-AT′, adopts an elongated structure with a twofold symmetry, resembling the crystal structures observed in the $(KS\text{-}LD\text{-}AT)_2$ fragments of 6-deoxyerythronolide B synthase (DEBS)(Tang et al., 2006).

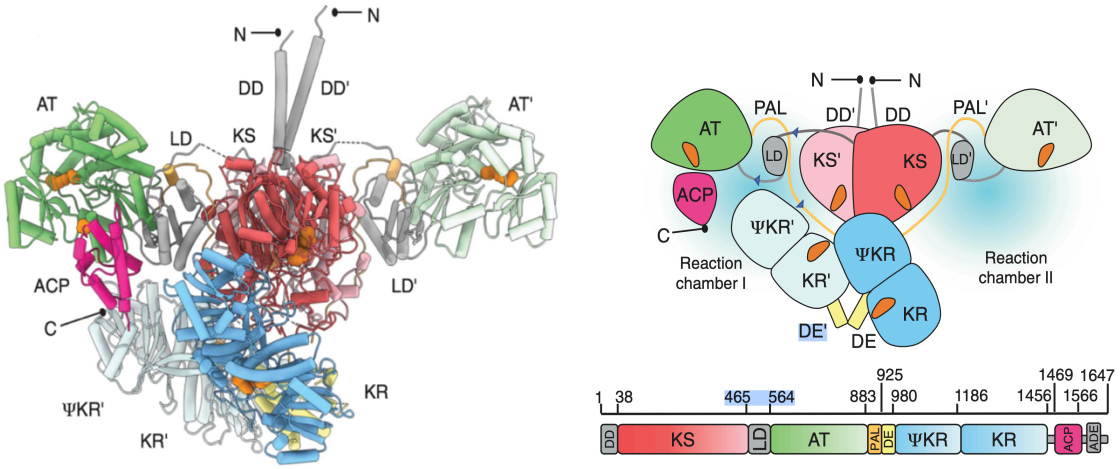


***Figure 4.*** *Crystal Structure of Lsd14 (left) - linear domain composition (right)*

Positioned beneath the $(KS\text{-}LD\text{-}AT)_2$ platform, the two Ketoreductase (KR) domains forms two reaction chambers, evoking a resemblance to the architecture of the porcine fatty acid synthase architecture. **(Figure 4)** (Bagde et al., 2021)

### 1.6. X-ray crystallography and protein crystallization

X-ray diffraction, usually called X-Ray crystallography, is a powerful non-destructive technique. By utilizing the interatomic spacing found in crystalline solids or crystallized biomolecules, this technique capitalizes on them as a diffraction gradient for X-ray light (Gawas et al., 2019; Parker, 2003). To solve a protein structure, thousands of 2D diffraction patterns need to be collected. The data collection method and the quantity of data needed depend on the specific characteristics of the crystal, such as its cell dimensions and symmetry. The location of atoms in the final structure is determined by calculating the electron density of the molecules within the crystal, derived from the intensities of the X-ray diffraction spots. (Dauter, 2017) The need for crystals in X-ray diffraction studies arises due to very weak scattering from individual atoms/molecules, whereas the crystals act like an amplifier increasing the scattering signal due the presence of multiple copies of molecules contained within the crystals. Undoubtedly, the most challenging and least understood aspect of protein crystallography is the growth of protein crystals that meet the criteria for high-quality structure determination, often serving as the primary bottleneck in the process. The principle of crystallization, of macromolecules is to take a solution of the sample at high concentration and induce it to come out of solution; if this process is too fast then precipitation will occur, but under the correct conditions crystals will grow (Chayen & Saridakis, 2008). The determination of these conditions establishes the step that limits the rate of progress and ultimately whether the project will be possible. The magnitude of the problem becomes apparent when

considering the numerous variables involved, including the selection and concentration of the precipitant, the buffer pH, the protein concentration, the temperature, the crystallization technique, and the possible inclusion of additives (McPherson & Gavira, 2014). In essence, the initial experiments will follow a trial-and-error approach, aiming to encompass a practical and comprehensive range of variables. During this stage, commercially available "crystal screen" packages are frequently employed. Each one usually consists of 96 solutions varying widely in precipitant, buffer, pH, and salt. These can then be set up using the techniques of sitting drop vapor diffusion. By employing this approach, a wide range of variables can be easily addressed, potentially resulting in the formation of high-quality crystals that can be utilized for the subsequent steps. (Benvenuti & Mangani, 2007)

# Materials and methods

## 2.1 Expression vectors

Custom-synthesized codon optimized DNA sequences for N-His-Lsd13, Lsd13-ACP and N-His-Lsd14 proteins cloned in pET28a(+) vector, N-terminal-TEV cleavable hexa-Histidine tagged Lsd14-KS-AT fragment cloned in pET28a(+)and tagless-Lsd13 and tagless-Lsd14 proteins cloned in pGEX-6P-1 were provided by GenScript®.

## 2.2. Chemical transformation of *E. coli* cells

The constructs were transformed into chemically competent BL21/BAP1 cells for protein expression and DH5α/TOP10F' cells for plasmid replication and extraction. Approximately 100ng of plasmid DNA was added to competent cell aliquot and mixed gently. The transformation mix was subjected to a 30-minute incubation on ice. Heat shock was given at 42°C for 30 seconds using Eppendorf ThermoMixer® after which the transformation mix was incubated in ice for 2-3 minutes, 200 uL of pre-warmed (37°C) LB media was added and the mixture was incubated at 37°C for 45 minutes. The transformed cells were spread on selective LB agar plates containing appropriate antibiotics and incubated at 37°C for 12 hours.

## 2.3. Protein expression in *E. coli* cells

Plasmids (pet28a+) expressing N-His-Lsd13, Lsd13-ACP-long, N-His-Lsd14 and Lsd14-KS-AT as N-terminal thrombin cleavable hexa-Histidine tagged constructs, and plasmids (pGEX-6P-1) expressing tagless-Lsd13 and tagless-Lsd14 as N-terminal GST fusion proteins with a PreScission protease site were expressed in BL21(DE3)/BAP1 *E. coli* cells. Expression culture (LB broth,

supplemented with 50µg/ml kanamycin for pET-28a(+) and 100µg/ml ampicillin for pGEX-6P-1) was inoculated with primary culture grown until $OD_{600}$ reached a value of 2 at 37°C, in the ratio 1:50. The expression culture grew until $OD_{600}$ reached a value of 0.6, after which the temperature of the incubator was switched to 18°C and were induced with 0.2mM IPTG. The cells were harvested after 18 hours by centrifugation at 6000xg for 20 minutes, and the cell pellets were stored at -80°C.

### 2.4. Protein purification

#### 2.4.1 Purification protocol Hexa-Histidine tagged proteins.

Cells from 1L expression culture were resuspended in 25ml lysis buffer (see table below), homogenized using sonication, and centrifuged at 30,000xg for 1 hour to clear the cell debris.
The clear supernatant was applied to IMAC (Immobilized Metal Affinity Chromatography) column charged with nickel ions, pre-equilibrated with IMAC buffer A (5mL Histrap HP columns GE Healthcare). Protein of interest was eluted with IMAC buffer B containing 500 mM imidazole, after washing the column with 50CV of 5% and 15% of buffer B respectively. The protein obtained was further purified using anion exchange chromatography (AEC). IMAC purified protein was applied to 5ml HiTrap Q-HP column GE healthcare upon dilution with AEC buffer A in a ratio of 1:5. Protein was eluted with a gradient of increasing percentage of AEC buffer B (high salt content, 1M NaCl) from 1%B to 50%B over 20 column volumes. AEC purified protein was further purified with SEC (Size Exclusion Chromatography) using Superdex200 Increase 10/300 GL column (GE Healthcare) equilibrated with SEC buffers giving the most homogeneous sample. The final pure protein was concentrated using MilliporeSigma™ Amicon™ Ultra-15 Centrifugal Filter Units

with a cellulose membrane with MWCOs of 10 kDa for Lsd13-ACp and 50 kDa for N-His-Lsd13/14.

**N-His-Lsd13-ACP-long:**

**Lysis buffer:** 50mM sodium phosphate pH 7.0, 0.5M NaCl, 10mM Imidazole, 20% glycerol, 0.5 mM PMSF

**IMAC-A:** 50mM sodium phosphate pH 7.0, 0.5M NaCl, 10mM Imidazole, 10% glycerol.

**IMAC-B:** 50mM sodium phosphate pH 7.0, 0.5M NaCl, 500mM Imidazole, 10% glycerol.

**SEC:** 25mM sodium phosphate pH 7.0, 0.5M NaCl.

**N-His-Lsd13, N-His-Lsd14-KS-AT:**

**Lysis buffer:** 20mM Sodium Phosphate, pH 7.0, 20% Glycerol, 300mM Sodium chloride, 0.5 mM PMSF

**IMAC-A:** 20mM Sodium Phosphate, pH 7.0, 10% Glycerol, 300mM Sodium chloride.

**IMAC-B:** 20mM Sodium Phosphate, pH 7.0, 10% Glycerol, 300mM Sodium chloride, 500 mM imidazole.

**AEC-A:** 50 mM Tris-HCl, 10% Glycerol, pH 8.5, 1mM DTT.

**AEC-B:** 50 mM Tris-HCl, 10% Glycerol, pH 8.5, 1M NaCl, 1mM DTT.

**SEC:** 25mM HEPES pH 7.5, 150mM NaCl, 1mM TCEP.

### 2.4.2 Purification protocol GST tagged/PreScission cleavage proteins.

Tagless-Lsd13 and tagless-Lsd14 cells from 1L expression culture were resuspended in 25ml lysis buffer (50mM sodium phosphate pH 7.0, 0.5M NaCl, 10mM Imidazole, 20% glycerol, 0.5 mM PMSF), homogenized using sonication, and centrifuged at 30,000xg for 1 hour to clear the cell

debris. The clear supernatant was applied over 1mL of equilibrated Glutathione resin and incubated at 4oC for 1-3 hours by continuous inverting. After the incubation time, spin down the resin in a centrifuge at 1500 RPM for 5 minutes at 4oC and discard the supernatant. Wash 3 times the resin with 20mLs of PBS (Phosphate Buffered Saline, pH 7.4) supplemented with 5mM BME. Resuspend the resin in 1mL of PreScission Cleavage Buffer (50 mM Tris-HCl pH 7.5, 150 mM NaCl, 1 mM EDTA, 1mM DTT.) and add sufficient PreScission protease. Incubate for 4 hours at 4oC by inverting, after remove the supernatant and dilute the eluted protein 5 times with Anion Exchange Buffer A (50mM Tris pH 8.5, 10% Glycerol, 1mM DTT.) and purify using Anion Exchange Chromatography (1ml MonoQ column 5/50 GL). Apply the protein to the column and elute with a gradient of 0 to 50% buffer B (50mM Tris pH 8.5, 10% Glycerol, 1mM DTT, 1M NaCl) over 20 column volumes using FPLCAEC purified protein was further purified with SEC (Size Exclusion Chromatography) using Superdex200 Increase 10/300 GL column (GE Healthcare) equilibrated with SEC buffer (25mM HEPES pH 7.5, 150mM NaCl, 1mM TCEP) giving the most homogeneous sample. The final pure protein was concentrated using MilliporeSigma™ Amicon™ Ultra-15 Centrifugal Filter Units.

**2.5. Crystallization trials.**

Initial crystallization screening experiments were set up for N-His-Lsd13, tagless-lsd13, using commercially available crystallization screens Morpheus I, II, III, LMB, PGA, JCSG+ and JG9 from Molecular Dimensions, MCSG Crystallization Suite and TOP96 from Anatrace, and PEGRxHT, Crystal Screen 1/2, PEG-Ion and Index from Hampton Research. The optimal protein concentration for crystallization set-up was determined using the PCTTM Pre-Crystallization test (Hampton Research). Using NT8 nanoliter-volume liquid handler robot 0.2µL of protein at two

different concentrations between 0.5-3mg/ml was mixed with 0.2µL of reservoir solution in a 96 well sitting drop plate and the plates were incubated at temperatures ranging from 10 to 18°C.

### 2.6. Protein concentration determination

Protein concentrations in this study were determined using an Eppendorf Biospectrophotometer Basic, measuring the absorbance at 280nm and considering the theoretical extinction coefficient calculated using ProtParam. The QuickStarTM Bradford Protein Assay was employed as a comparative control for validation purposes.

### 2.7. Surface Plasmon Resonance measurements

Sensor chips (NTA) were purchased from Nicoya Lifesciences. SPR experiments were performed on a Nicoya OpenSPR instrument. Running buffer for SPR was 25 mM HEPES, pH 7.5, 0.15 M NaCl. The surface was prepared for immobilization of N-His-Lsd13 by activating with 50 mM $NiCl_2$ in running buffer. N-His-Lsd13 concentration used for loading was 50mM for all the experiments. Kinetic data analysis was carried out using TraceDrawer Analysis Software from Nicoya.

# Results and discussion

## 3.1. Expression of recombinant polyketide synthases

N-His-Lsd13 (119kDa), tagless-Lsd14 (174kDa), N-His-Lsd13-ACP-long (12kDa) and N-His-Lsd14-KS-AT (98KDa) polyketides synthases were successfully expressed in competent *E. Coli* BL21-D3 cells. Expression for all proteins was done adding 0.2 M IPTG at 18 Celsius degrees for 18 hours.

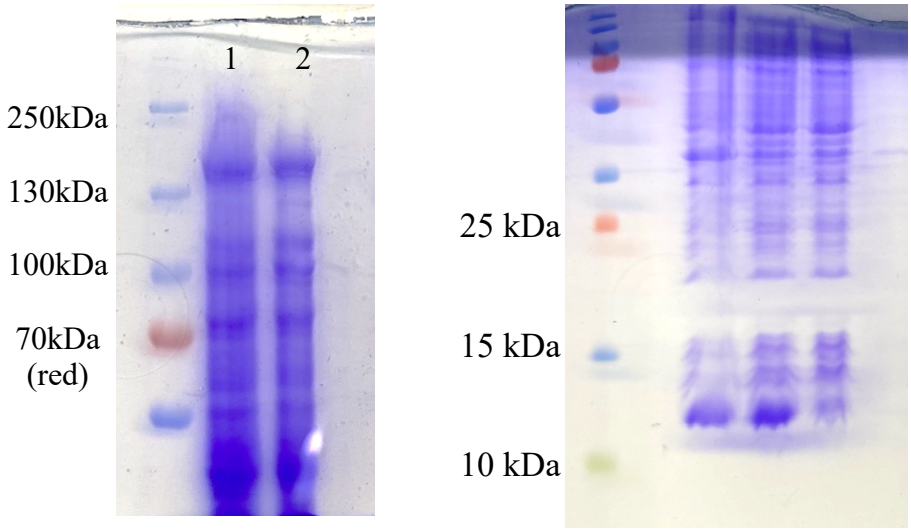


***Figure 5.*** *Lsd13 (lane 1) and Lsd14 (lane 2) expression (right) / Lsd13-ACP expression SDS-gel (left)*

The expression-solubility levels of N-His-Lsd13, tagless-Lsd14, N-His-Lsd13-ACP-long and N-His-Lsd14-KS-AT were satisfactory, allowing us to continue with the purification of these polyketide synthases for protein crystallization trials.

### 3.2. Purification of recombinant polyketide synthases

The purification procedure for N-His-Lsd13, tagless-Lsd14, N-His-Lsd13-ACP-long and N-His-Lsd14-KS-AT has been standardized. The steps involved are immobilized metal affinity chromatography (IMAC) or Glutathione-Agarose affinity chromatography (Glu-AC) for tagless-Lsd14, anion exchange chromatography (AEC) and size exclusion chromatography (SEC) as discussed in detail in section 2.4.

**Immobilized Metal Affinity Chromatography (IMAC)**

All the proteins and fragments in this study (except tagless-Lsd14) were expressed as N-terminal hexa-Histidine tagged constructs to aid in purification using IMAC. The Histidine residues in the His-tag bind to nickel ions immobilized on a stationary matrix or lose resin. Non-specifically or weakly bound impurity proteins are eluted upon washing the matrix with buffer containing low concentrations of imidazole which binds competitively to the immobilized nickel ions on the matrix. His-tagged protein can then be eluted using higher concentration of imidazole in the elution buffer. The binding of N-His-Lsd13, N-His-Lsd13-ACP-long and N-His-Lsd14-KS-AT to the IMAC column was optimized by changing the sodium chloride concentration or pH in the IMAC buffer.

For N-His-Lsd13 and H-His-Lsd14-KS-AT, further purification of the protein was necessary to get high quality protein for crystallographic studies since the IMAC step purity was not enough. Hence, IMAC purified protein was further subjected to Anion Exchange Chromatography. In N-His-Lsd13-ACP-long purity after IMAC step was above 95%, for this reason we only did one additional SEC purification step for buffer exchange and protein homogeneity.

**Glutathione-Agarose Affinity chromatography (Glu-AC) for tagless-LSd14**

The Glutathione Agarose is used for purifying GST-fusion proteins from cellular lysates. Glutathione is linked by its central sulfhydryl with a 12-atom spacer, which minimizes steric hindrance. Purification of GST-fusion proteins using glutathione agarose beads is well documented and provides an easy-to-use, one-step, high purity affinity purification. The bound GST-fusion proteins are eluted using a buffer containing reduced glutathione, or the fusion protein can be cleaved at the GST tag using thrombin, HRV 3C protease, or Factor Xa.

PreScission Protease is a genetically engineered fusion protein of human rhinovirus 3C protease and glutathione S transferase (**GST**). PreScission protease specifically cleaves between the Gln and Gly residues of the recognition sequence LeuGluValLeuPheGln/GlyPro.

Lsd14-GST tagged protein was designed to do an affinity purification/cleavages reaction at the same step. The clear lysate is mixed with the glutathione resin to specifically bind the GST-tagged protein, this step was optimized changing the time, amount of resin and inverting speed. Once the protein is bind to the resin, an enough amount of PreScission Protease is added to cleavage the HRV-3C site, getting the un-tagged protein in solution, for further purification steps.

**Anion Exchange Chromatography (AEC)**

Proteins can be separated using ion-exchange chromatography based on the net surface charge. Anion exchange chromatography involves use of a positively charged stationary phase and hence proteins with negative net surface charge can bind to the stationary phase. At a given pH, proteins with different iso-electric point (Pi) values will have different surface charge and can be separated using ion-exchange chromatography based on their affinity to the charged stationary phase upon

application of a salt gradient. Proteins having high affinity to the ion exchange matrix will elute at high ionic strength, that can be controlled in the elution buffer adding NaCl.

**Size exclusion chromatography (SEC)**

AEC purified protein was further subjected to Size exclusion chromatography to separate aggregates and to get a homogenous protein sample for crystallographic studies.

### 3.3.1 N-His-Lsd13 purification

**Lsd13** is a homodimer protein with a length: 1,113 Aa, Mass (Da): 119,270, Theoretical pI: 5.16 and the instability index (II) is computed to be 38.65, this classifies the protein as stable. A clear lysate was obtained using this lysis buffer: 20mM Sodium Phosphate, pH 7.0, 20% Glycerol, 300mM Sodium chloride, 0.5 mM PMSF. The lysate was loaded into the 5mL Histrap HP column at a flow rate of 3mg/ml adding 5% of buffer B containing imidazole to avoid non-specific binding of other proteins to the column. Protein was eluted at 50% of buffer B containing 500 mM imidazole **(Figure 6)**.

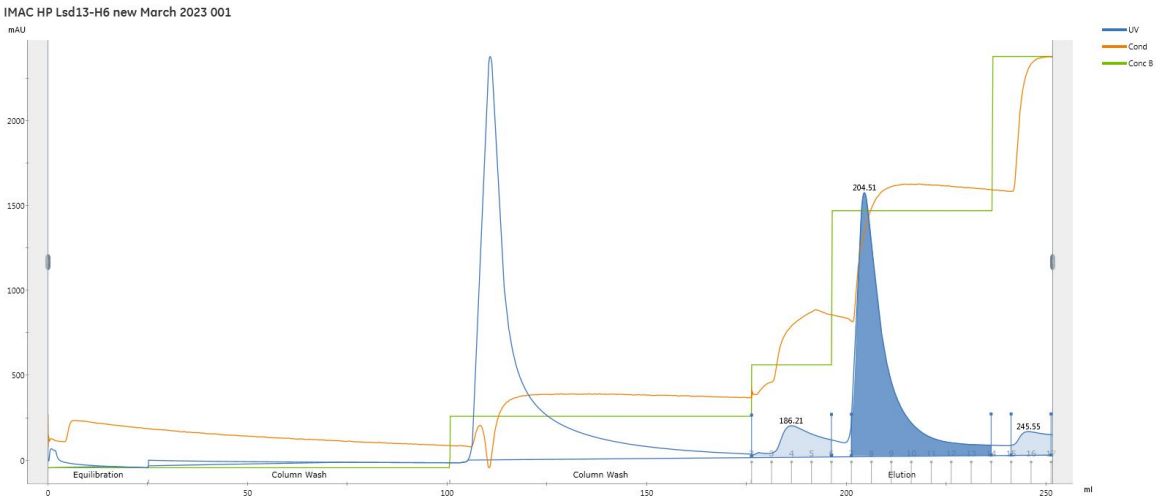


***Figure 6**. Immobilized Metal Affinity chromatogram N-His-Lsd13.*

The resulting single peak was further diluted up to 5 times with AEC buffer A to low the salt concentration and promote the binding to the Anion Exchange column. N-His-Lsd13 was eluted using AEC buffer B with 1 M sodium chloride concentration with a gradient program from 30% to 75%. **(Figure 7)** Size exclusion chromatography was archived after concentrating down to a volume that allowed several injections of 250 uL into the Superdex200 Increase 10/300 GL column (GE Healthcare) as described in section 2.4. **(Figure 8)**

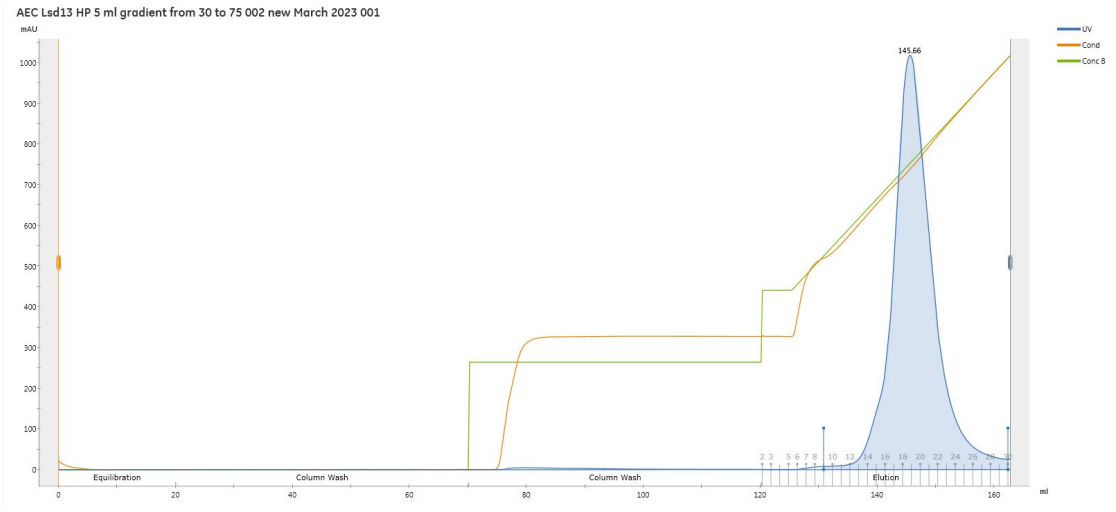


***Figure 7****. Anion Exchange chromatogram N-His-Lsd13.*

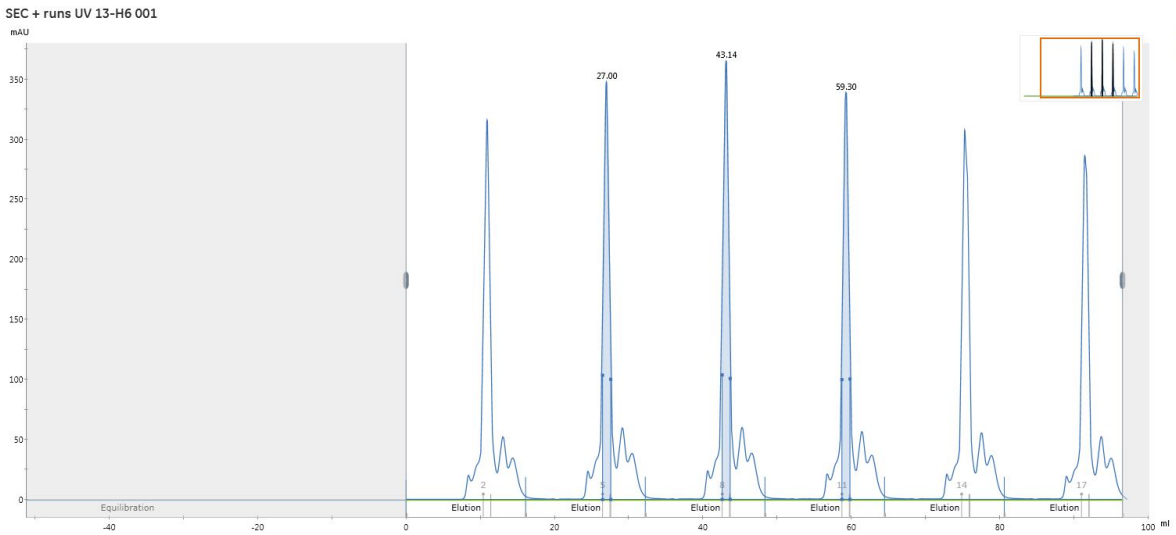


***Figure 8.*** *Size exclusion chromatogram N-His-Lsd13.*

The size exclusion program was settled to collect above 100 mAU UV units to avoid collecting the other small peaks around the peak of our protein, leading to a higher purity of our final protein solution. Our final solution was subjected to several tests to check homogeneity and dimeric composition. First the protein solution was re-injected to the size exclusion column leading to a highly symmetric single peak with an asymmetry 10% value of 1.62. **(Figure 9)**

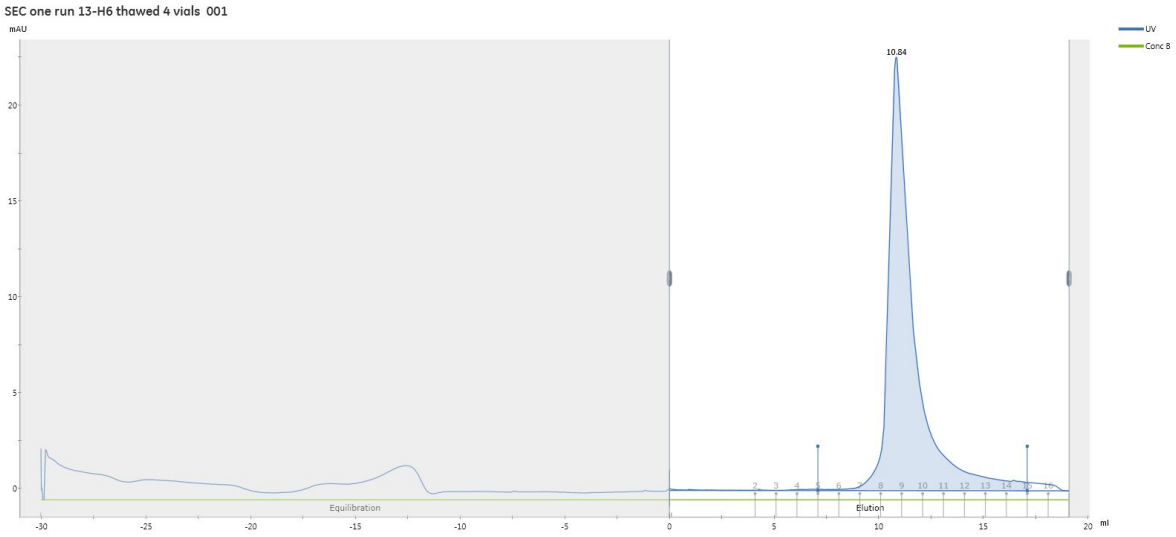


***Figure 9.*** *Size exclusion chromatogram pure N-His-Lsd13.*

Through Dynamic Light Scattering (DLS) measurements it was confirmed that our pure protein solution is completely homogeneous having a single population on the dimer state. **(Figure 10)**

| | | Size (d.nm): | % Volume: | St Dev (d.nm): |
|---|---|---|---|---|
| Z-Average (d.nm): 22.42 | Peak 1: | 14.09 | 99.9 | 4.883 |
| PdI: 0.217 | Peak 2: | 5078 | 0.0 | 783.1 |
| Intercept: 0.843 | Peak 3: | 201.8 | 0.0 | 61.54 |

Result quality : Refer to quality report

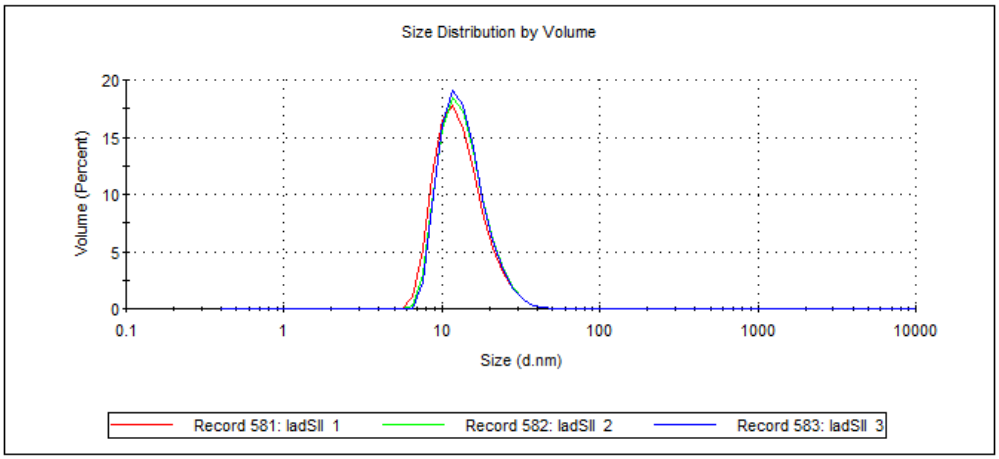


***Figure 10.*** *Dynamic Light Scattering chromatogram pure N-His-Lsd13.*

All fractions were analyzed by SDS-gel, leading to a final pure protein **(Figure 11)**, and with an average yield of **1.5-2 mg** per 4 liters of induced cells.

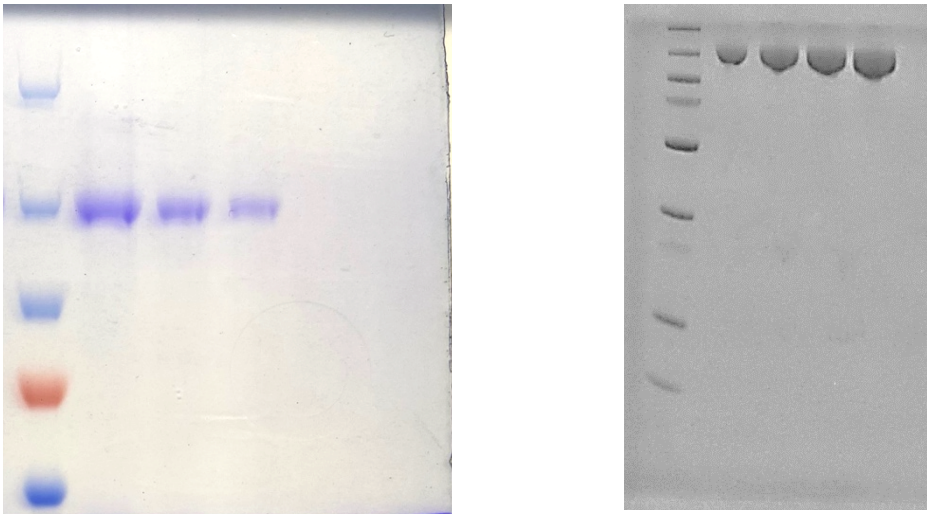

***Figure 11****. 7.5/3.5% SDS gel (left) and 12/4% SDS gel (right) of pure N-His-Lsd13.*

After the size exclusion purification step a clear-homogeneous solution of the protein was obtained, and after concentrated was flash freezed to further be use it for crystallization experiments. This purification is completely reproducible, leading to good yield and purity, and the chromatogram shows are representative of all the purifications done until this date.

### 3.3.2 N-His-Lsd13-ACP-long purification

Lsd13-ACP is the ACP domain fragment of Lsd13 protein with a length: 121 Aa, Mass (Da): 12,980; Theoretical pI: 6.02 and the instability index (II) is computed to be 34.12, this classifies the protein as stable.

A clear lysate was obtained using this lysis buffer: Phosphate Buffered Saline, pH 7.0, 500 mM NaCl, 20% Glycerol, then was loaded into a IMAC Nickel column and further eluted with IMAC buffer B containing 250 mM imidazole **(Figure 12).**

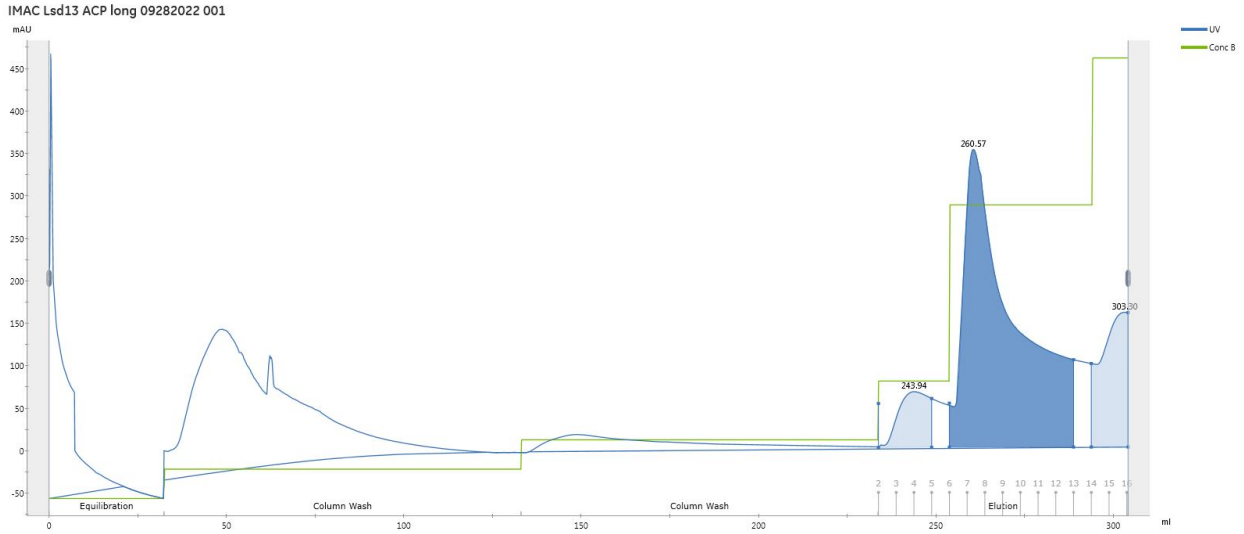


***Figure 12.*** *Immobilized Metal Affinity chromatogram N-His-Lsd13-ACP-long.*

A single peak was obtained leading to a pure protein fraction, that was further purified using Size exclusion chromatography using IMAC A buffer as SEC buffer. Concentrating down to a volume

that allowed several injections of 250 uL into the Superdex75 Increase 10/30 GL column (GE Healthcare) as described in section 2.4. **(Figure 13)**

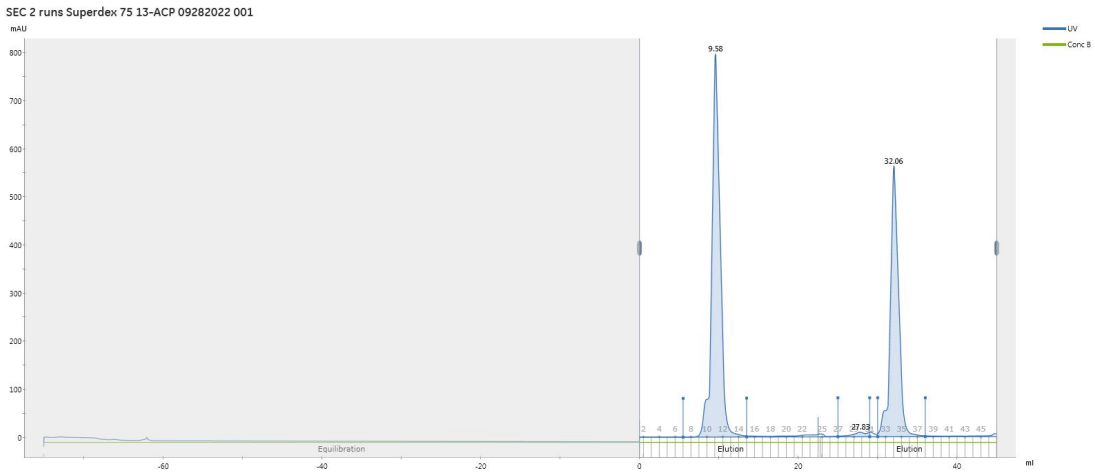


***Figure 13**. Size Exclusion chromatogram N-His-Lsd13-ACP-long.*

All fractions were analyzed by SDS-gel, leading to a final pure protein **(Figure 14)**, and with an average yield of **3-4 mg** per 2 liters of induced cells.

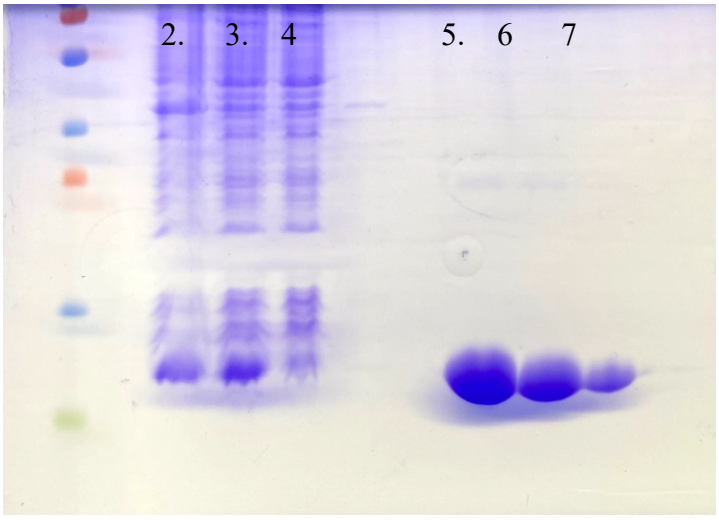


1- Protein ladder (2 color ladder)

2- Expression of Lsd13-ACP after IPTG

3- Expression of Lsd13-ACP after IPTG

4- BL21 cells before expression induction with IPTG.

5- To 7- Pure N-His-Lsd13-ACP

***Figure 14**. 12/4% SDS gel of pure N-His-Lsd13-ACP.*

After the size exclusion purification step a clear-homogeneous solution of the protein was obtained, and after concentrated was flash freezed to further be use it for crystallization experiments. This purification is completely reproducible, leading to good yield and purity, and the chromatogram shows are representative of all the purifications done until this date.

### 3.3.3 Tagless-Lsd14 purification

**Lsd14** is a homodimer protein with a length: 1,647 Aa, Mass (Da): 173,494, Theoretical pI: 4.92 and the instability index (II) is computed to be 36.89, this classifies the protein as stable.

A clear lysate was obtained using this lysis buffer: Phosphate Buffered Saline, pH 7.4, 20% Glycerol, 5mM BME, and it was mixed by inverting for 4 hours with 1 ml of equilibrated glutathione resin. After several cycles of washes was carried out the cleavage reaction was performed using PreScission enzyme in buffer: 50 mM Tris-HCl pH 7.5, 150 mM NaCl, 1 mM EDTA, 1mM DTT. A clear solution of the non-tagged protein was obtained and further diluted up to 5 times with AEC buffer A (50mM TrisHCl pH = 8.5, 10% glycerol) to low the salt concentration and promote the binding to the Anion Exchange column. Tagless protein was eluted using a gradient from 30% to 75% AEC buffer B including 1M sodium chloride salt concentration. **(Figure 15)**

Fractions were concentrated to a volume that allowed several injections of 250 uL into the Superdex200 Increase 10/300 GL column (GE Healthcare) as described in section 2.4. **(Figure 16)**

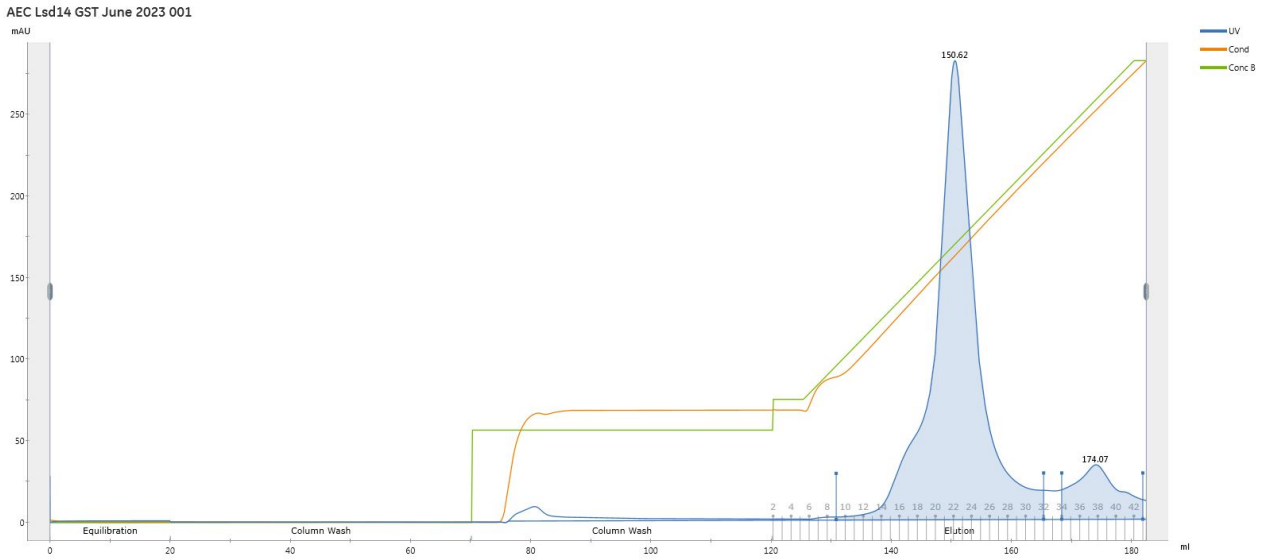


***Figure 15**. Anion Exchange chromatogram tagless-Lsd14.*

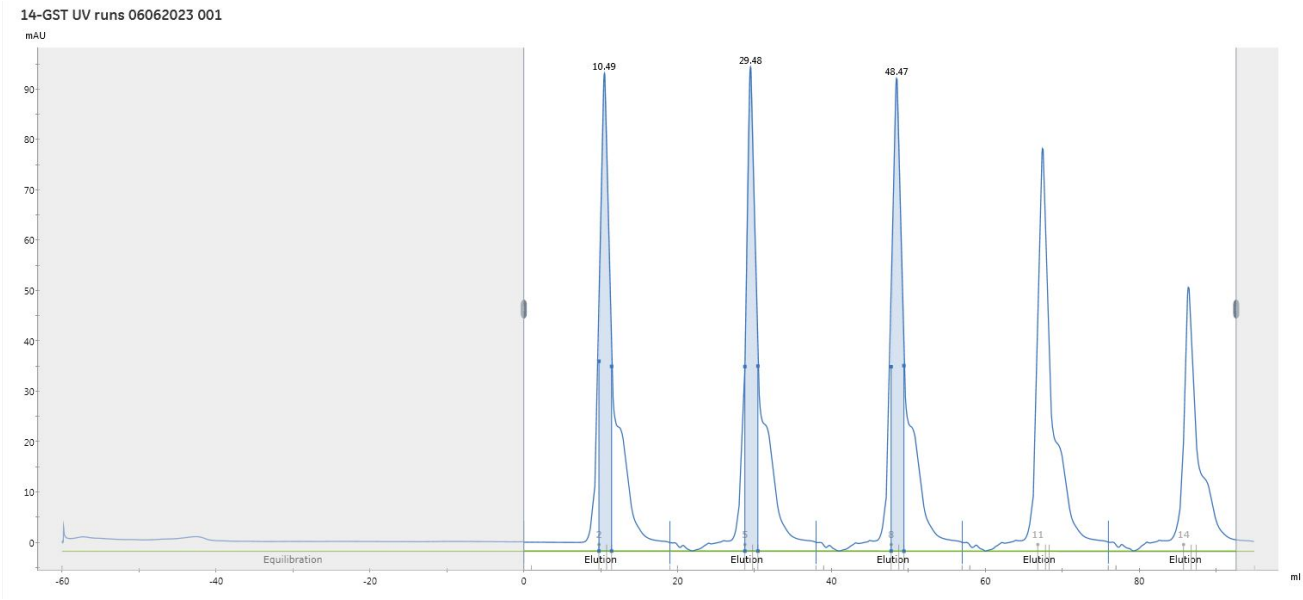


***Figure 16.** Size exclusion chromatogram tagless-Lsd14.*

The size exclusion program was settled to collect above 40 mAU UV units to avoid collecting the shoulder in the right of the peak leading to a higher purity of our final protein solution. Our final solution was subjected to several tests to check homogeneity and dimeric composition. First the

protein solution was re-injected to the size exclusion column leading to a highly symmetric single peak with an asymmetry 10% value of 1.70. **(Figure 17)**

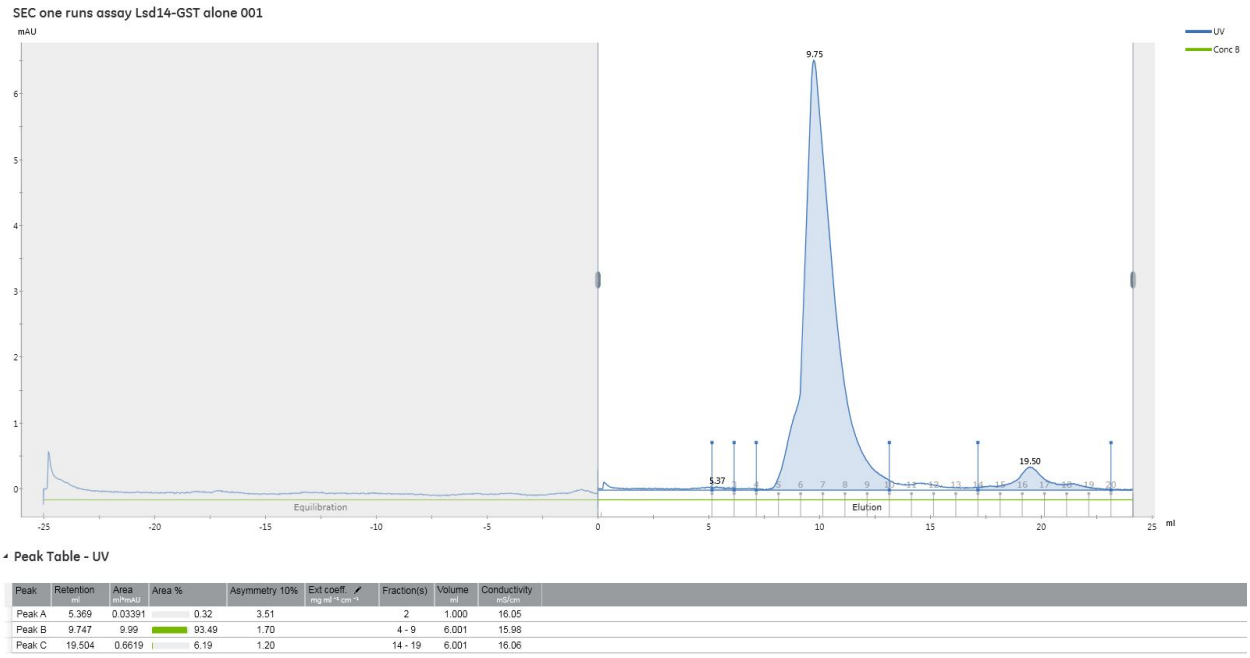


| Peak | Retention ml | Area mHmAU | Area % | Asymmetry 10% | Ext.coeff. mg ml⁻¹ cm⁻¹ | Fraction(s) | Volume ml | Conductivity mS/cm |
|---|---|---|---|---|---|---|---|---|
| Peak A | 5.369 | 0.03391 | 0.32 | 3.51 | | 2 | 1.000 | 16.05 |
| Peak B | 9.747 | 9.99 | 93.49 | 1.70 | | 4 - 9 | 6.001 | 15.98 |
| Peak C | 19.504 | 0.6619 | 6.19 | 1.20 | | 14 - 19 | 6.001 | 16.06 |

***Figure 17.*** *Size exclusion chromatogram pure tagless-Lsd14.*

All fractions were analyzed by SDS-gel, leading to a final pure protein (Figure 18), and with an average yield of **1.0 - 1.5 mg** per 4 liters of induced cells. After the size exclusion purification step a clear-homogeneous solution of the protein was obtained, and after concentrated was flash freezed to further be use it for crystallization experiments.

This purification is completely reproducible, leading to good yield and purity, and the chromatogram shows are representative of all the purifications done until this date.

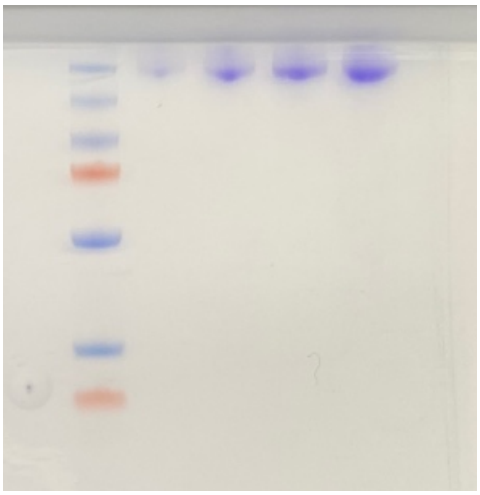

***Figure 18.*** *12/4% SDS gel of pure tagless-Lsd14.*

### 3.3.4 Tagless-Lsd14-KS-AT purification

**Lsd14-KS-AT** is the KS-AT domain fragment of Lsd14 protein with a length: 915 Aa, Mass (Da): 97,214, Theoretical pI: 5.46 and the instability index (II) is computed to be 38.18, this classifies the protein as stable.

A clear lysate was obtained using Lysis buffer: Phosphate Buffered Saline, pH 7.0, 300 mM NaCl, 20% Glycerol, then was loaded into a IMAC Nickel column and further eluted with IMAC buffer B containing 250 mM imidazole. **(Figure 19)**

A clear solution of the tagged protein was obtained and further diluted up to 5 times with AEC buffer A (50mM TrisHCl pH = 8.5, 10% glycerol) to low the salt concentration and promote the binding to the Anion Exchange column. Tagless protein was eluted using a gradient from 30% to 75% AEC buffer B including 1M sodium chloride salt concentration. **(Figure 20)**

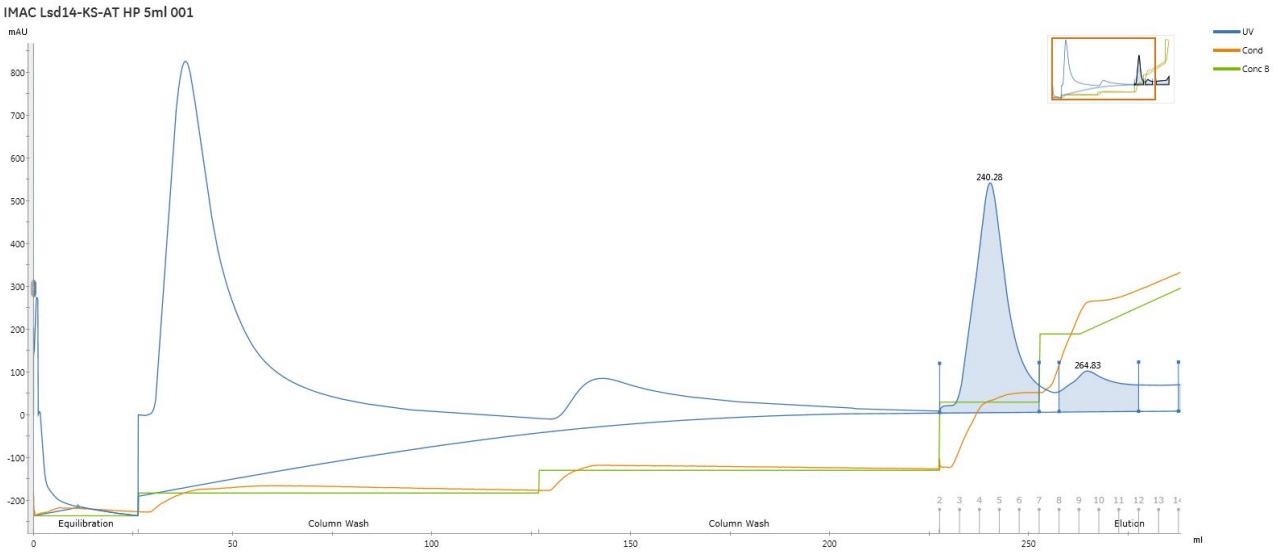


***Figure 19.*** *Immobilized Metal Affinity chromatogram N-His-Lsd14-KS-AT.*

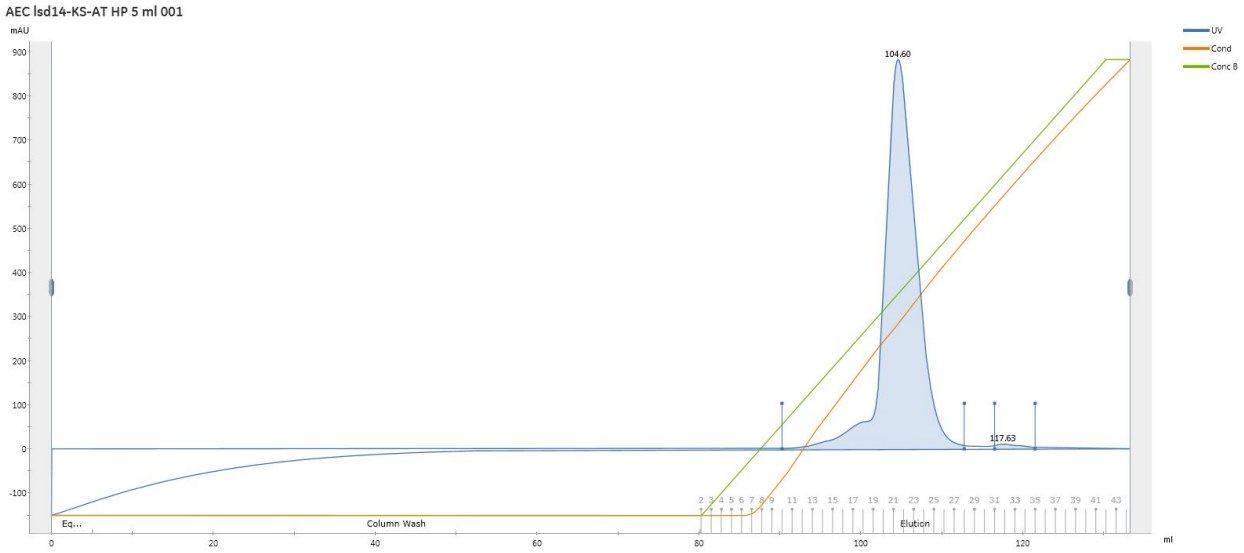


***Figure 20****. Anion Exchange chromatogram N-His-Lsd14-KS-AT.*

Fractions from AEC purification step were concentrated to 100uL and settled the cleavage reaction. Following the TEV cleavage typical reaction set-up to a total volume of 100 uL, 50 ug of pure protein was combined with 10 uL TEV protease reaction buffer 10X and 2 uL of TEV Protease. The mixture was incubated at 4 Celsius degrees overnight and further applied into the Superdex75 Increase 10/30 GL column (GE Healthcare) as described in section 2.4. **(Figure 21)**

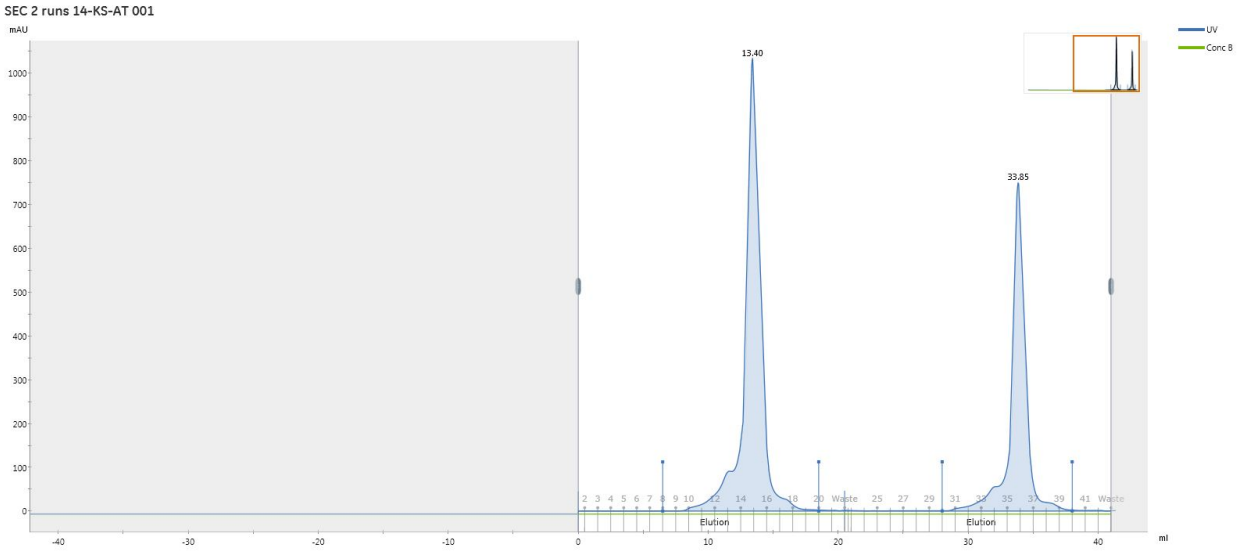


***Figure 21.*** *Size exclusion chromatogram tagless-Lsd14-KS-AT.*

All fractions were analyzed by SDS-gel, leading to a final pure protein **(Figure 22)**, and with an average yield of **1.5-2 mg** per 4 liters of induced cells. After the size exclusion purification step a clear-homogeneous solution of the protein was obtained, and after concentrated was flash freezed to further be use it for crystallization experiments.

1. 2. 3. 4.

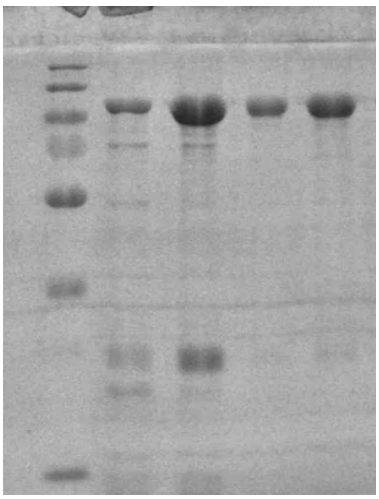

1 – IMAC sample

2 – AEC sample

3,4 – SEC tagless 14-KS-AT pure sample

***Figure 22****. 12/4% SDS gel of pure tagless-Lsd14-KS-AT.*

### 3.4. Crystallization experiments of N-His-Lsd13

Lsd13 structure will provide information about how PKSs structure is driven, if this is in fact a build-up system where just domain are added to a fixed structure or adding domains will completely change the structure. Crystallization experiment started after N-His-Lsd13 purity above 95% and homogeneity of the solution was confirmed. Crystallization experiments were performed using a sitting drop vapor diffusion method with help of the automated NT8 robot from FORMULATRIX® and commercial screens. The program was settled for a drop size of 0.4 uL using INTELLI-3 drops plates.

Lsd14 belongs to the same pathway and the identity to our protein Lsd13 is 79.4%, considering the difference in length, this value is really high. In our first crystallization experiments we used the same buffer used for Lsd14 crystallization: 25mM HEPES pH = 7.2, 150 mM NaCl and 1mM TCEP. Optimal protein concentration was determined using the PCT$^{TM}$ Pre-Crystallization test (Hampton Research). We didn't get any potential hit in this experiment, and we started changing some variables. First, we performed several experiments ranging protein concentration from 1 mg/ml to 6.5 mg/ml, these changes didn't lead to any potential crystal hit. Next, we changed the SEC buffer to 25mM TrisHCl pH = 8.0, 150 mM NaCl, 1mM TCEP; and 10 mM Sodium Phosphate, pH = 7.0, 150mM NaCl, 1mM TCEP, but these buffers with different pH didn't lead to any potential crystal hit.

Reductive alkylation of proteins is a wide used protocol to change proteins properties like solubility, isoelectric point and hydropathy by alkylation of lysine residues. Reductive alkylation modification may promote crystallization via improved crystal packing. Pure N-His-Lsd13 protein was subjected to reductive alkylation modification with methyl **(Figure 23)**, ethyl **(Figure 24)** and isopropyl **(Figure 25)** groups in the lysine residues, using the Reductive Alkylation kit from

Hampton Research. Purity of the final modified protein was checked by SDS gel and compared with non-modified protein. **(Figure 26)**

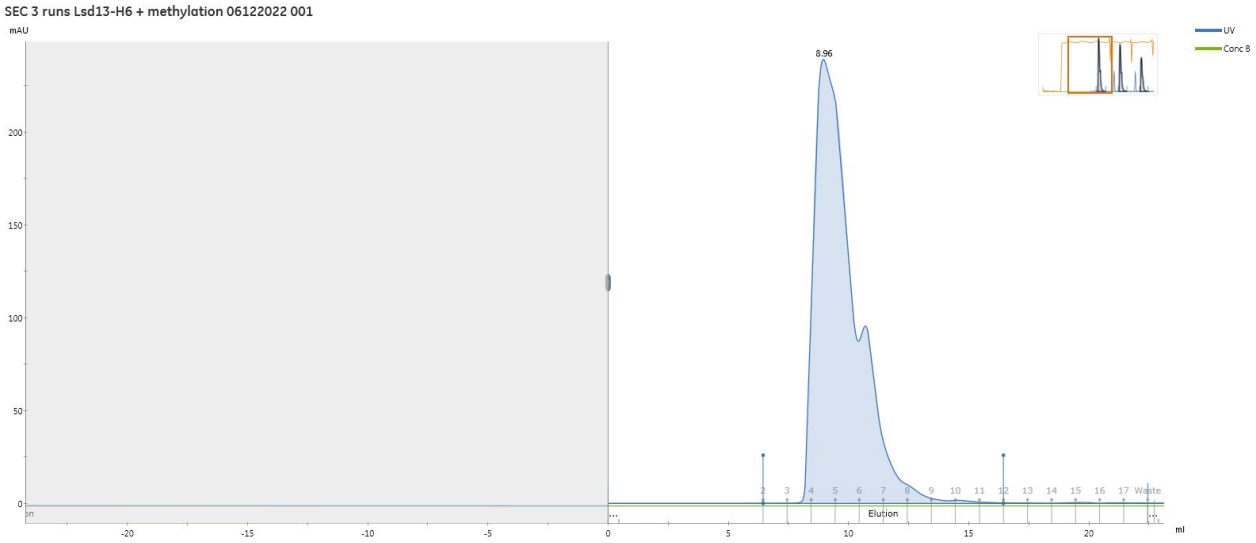


***Figure 23.*** *Size exclusion chromatogram methylated-Lsd13.*

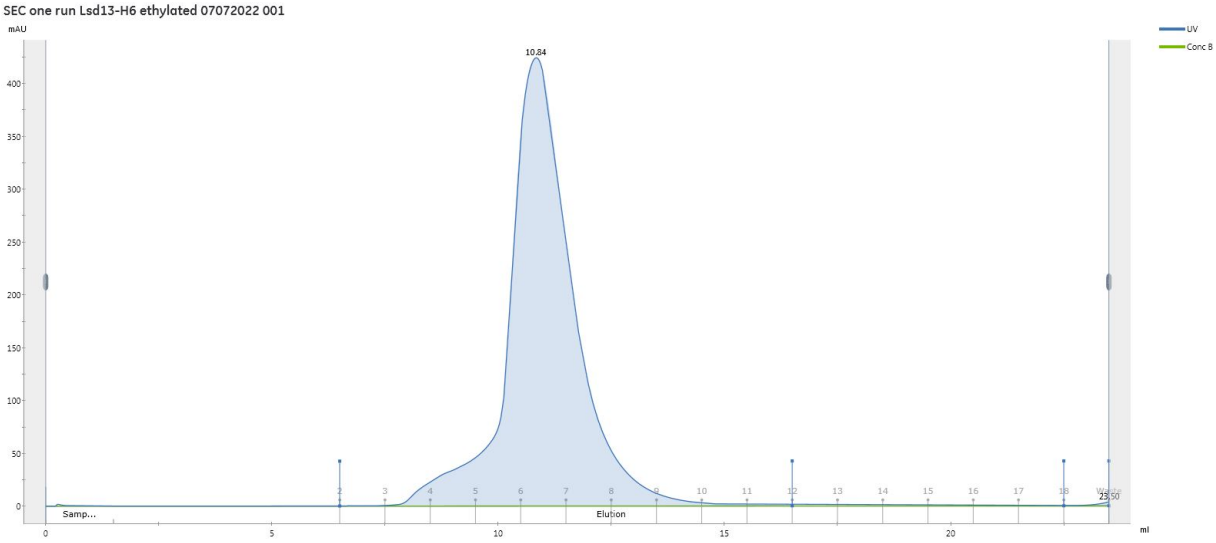


***Figure 24.*** *Size exclusion chromatogram ethylated-Lsd13.*

Crystallization experiments were settled using all three alkylated proteins, but no potential hits were detected after one year at two different temperatures 10 and 18 Celsius degrees, at three different protein concentration 1.0 mg/mL, 2.0 mg/mL and 3.0 mg/mL.

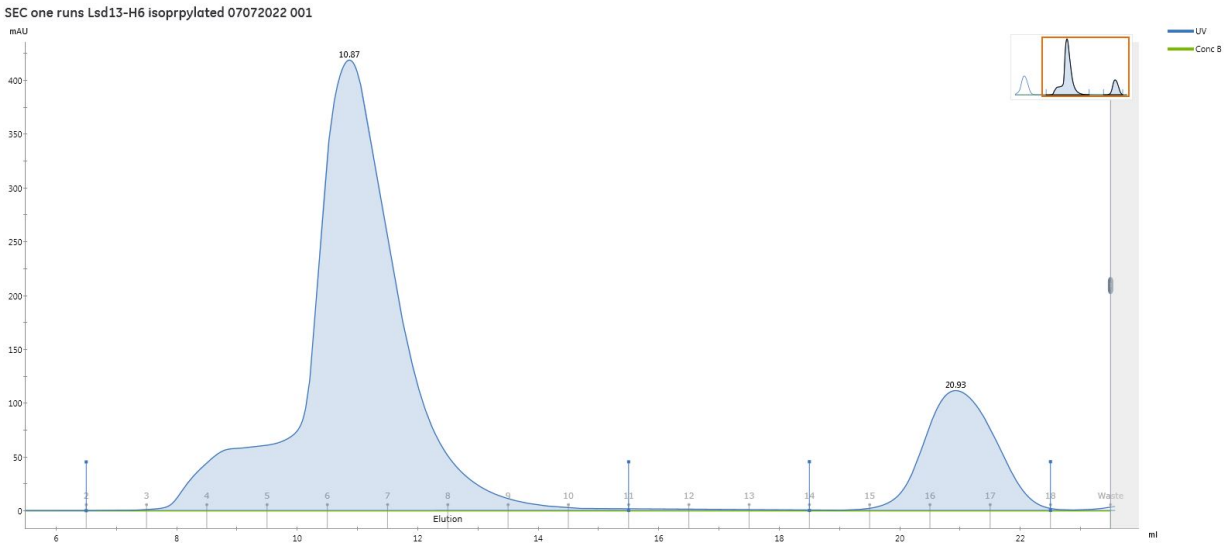


***Figure 25.*** *Size exclusion chromatogram isopropylated-Lsd13.*

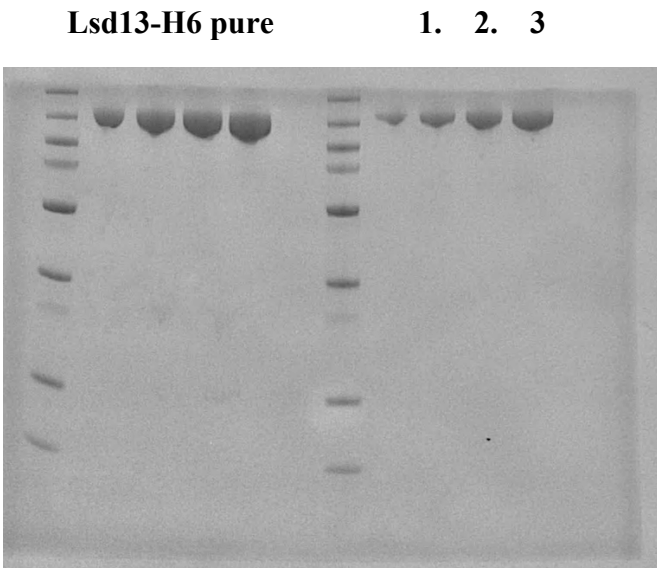


1 – methylated-Lsd13

2 – ethylated-Lsd13

3 – isopropylated-Lsd13

***Figure 26.*** *12/4% SDS gel N-His-Lsd13 before / after reductive alkylation modification.*

Another strategy to archive a protein crystal is to add molecules that bind to the protein or interact in any way that could make the structure more rigid or lock it in a certain conformation. Cerulenin is a known fungal antibiotic that inhibits the condensing enzymes involved in the polyketide biosynthesis. Since Cerulenin binds to the Keto-Synthase (KS) domain will make the protein more rigid and will promote crystallization, this is our hypothesis for this experiment. Following the same methodology we used Malonyl-Coenzyme A, the extender unit selected by the Acyltransferase (AT) domain.

Both experiments were done following several protocols reported in the literature, incubating the protein with the molecule (Cerulenin or Malonyl-CoA) and after performing SEC to remove the access, or we added the molecule directly to the SEC buffer **(Figure 27).**

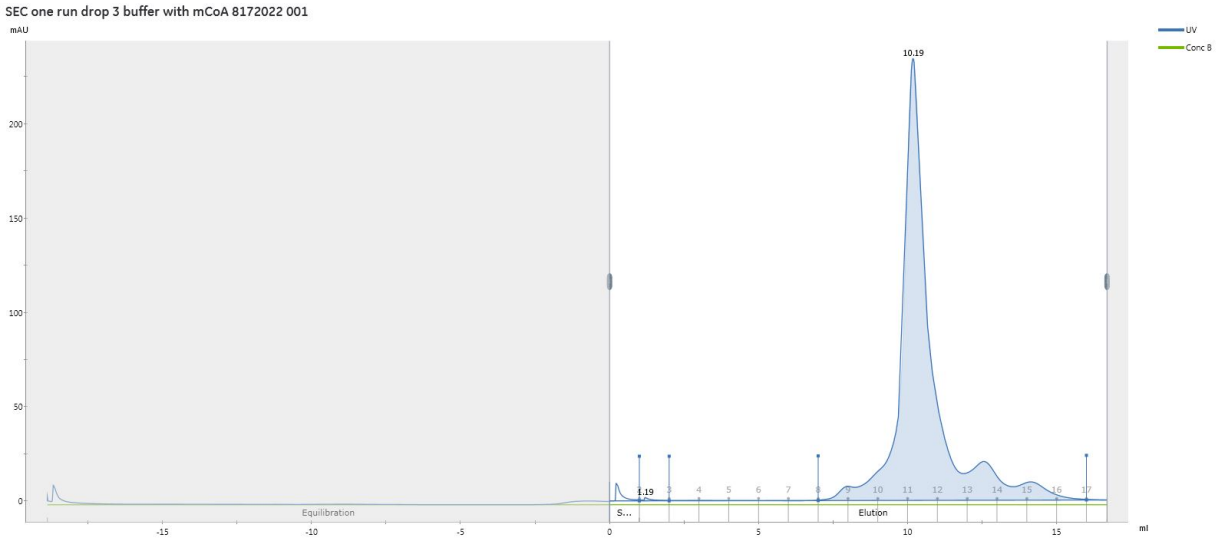


***Figure 27.*** *Size exclusion chromatogram N-His-Lsd13 (buffer containing mCoA).*

At the end none of the molecules or different methodology led to any potential protein crystal.

In this case our last experiment was to change the crystallization method. So far, all the experiments were done by sitting drop diffusion method using the NT8 robot. There are several reports that some proteins prefer a specific crystallization method, another option was to try out micro-batch under oil method. In this method crystallization takes place by direct contact of the protein solution with the precipitant agent and salt, not by a concentration process like in vapor diffusion method.

The National Crystallization Center is an institution that supports academic by providing a unique protein crystallization service for structural biology. Crystallization experiments are done at this center using micro-batch under oil method and utilizing an in-house optimized cocktail of 1,536 different chemical conditions.

We submitted a sample of freshly purified N-His-Lsd13 for crystallization experiments, with a protein concentration of 1.5 mg/ml at 14 Celsius degrees. Crystallization screening at the National Crystallization Center at HWI was supported through NIH grant R24GM141256**.** After 6 weeks we got the pictures for a potential protein crystal hit that was confirmed since it's produced UV-TPEF signal, considering that Lsd13 has 18 tryptophan in the sequence.

After a potential hit was archived, we started the process of replicate the hit using both vapor diffusion and micro-batch under oil method. The crystallization condition used to obtain the initial hit is well 1338: 0.1 M TRIS pH = 8.5, 1.5 M Ammonium Sulfate and 12% Glycerol (v/v).

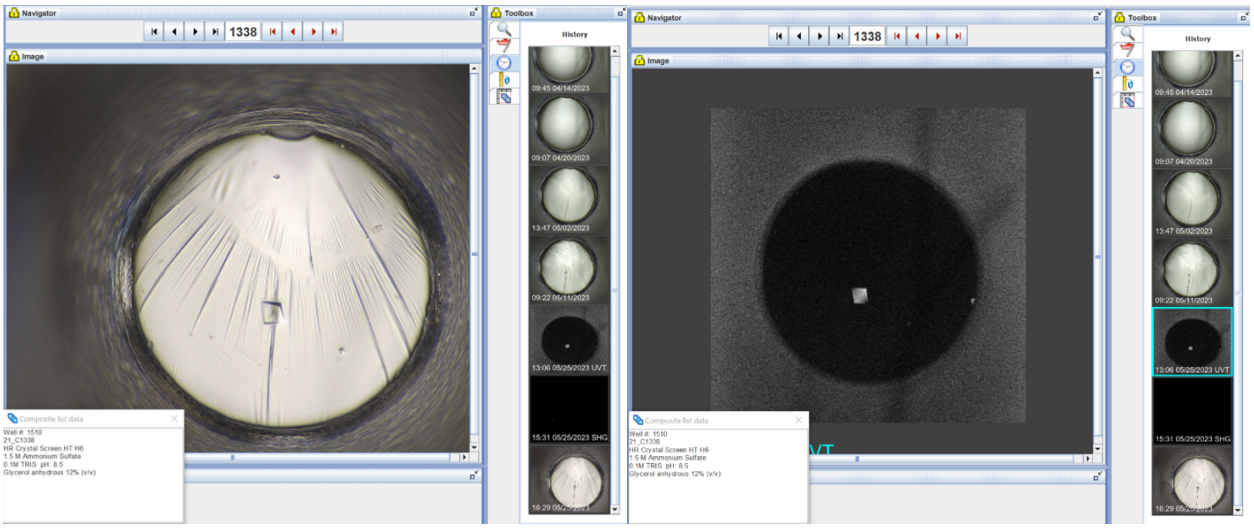


***Figure 28.*** *Lsd13 potential hit - Visual (brightfield) (left) and UV-Two Photon Excited Fluorescence (UV-TPEF) (right) images.*

### 3.5. Crystallization experiments of N-His-Lsd13/tagless-Lsd14 complex

In a polyketide biosynthesis pathway several synthases come together to grow the polyketide chain and generate the final structure. Still it's a mystery how different polyketide synthases interact to each other and what are the contact point in the interface formed in the complex. Even is not known if the polyketide synthases comes together to form a complex and the chain transfer process will take place after or if the complex formation is forced by the chain transfer process.

Before starting Lsd13-Lsd14 complex crystallization experiments it was needed to confirm the interaction between these two proteins at these conditions, like buffer pH and salt concentration. The first experiment that we performed to check this fact was a pull-down assay using Nickel beads. Our system is composed by N-His-Lsd13 and tagless-Lsd14, in theory, tagless-Lsd14 should not bind or interact with the Nickel resin. This was confirmed and even in our process we did washes using 10% buffer B to elute any non-specific possible interaction of tagless-Lsd14 with

the Nickel resin. Complex was incubated for 15 min, and further eluted using IMAC buffer B containing imidazole. Elution conditions used were the same as IMAC elution of N-His-Lsd13.

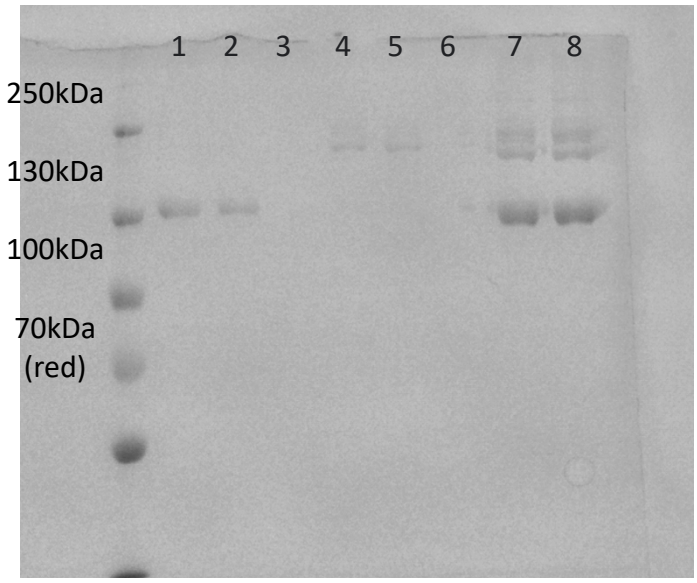


1. Went through the resin N-His-Lsd13
2. Wash #1
3. Wash #2 **(no protein coming out)**
4. Went through tagless-Lsd14.
5. Wash #1
6. Wash #2 **(10% buffer B)**
7. 8. Complex eluted **(both proteins)**

***Figure 29.*** *Pull-down assay N-His-Lsd13 and tagless-Lsd14.*

Pull-down assay is a great technique to determine interaction between two proteins since is easy to perform in the laboratory, but it will not provide any numerical information.

To get a binding affinity value between these two proteins we used Surface Plasmon Resonance technique, using the same construct binding N-His-Lsd13 to a Nickel covered sensor. Several experiments were performed to reach the Rmax for the ligand N-His-Lsd13 to the sensor chip; we measured KD's for the partner tagless-Lsd14 full length PKS at concentrations between 50 to 600 mg/ml. From SPR measurements we got a 35.2 nM binding affinity using the OneToOne fitting method. This affinity is sufficient to initiate crystallization experiments for the complex, utilizing N-His-Lsd13 and tagless-Lsd14. Notably, this value aligns with the KD values previously reported by other research groups for fragments of continuous PKSs.

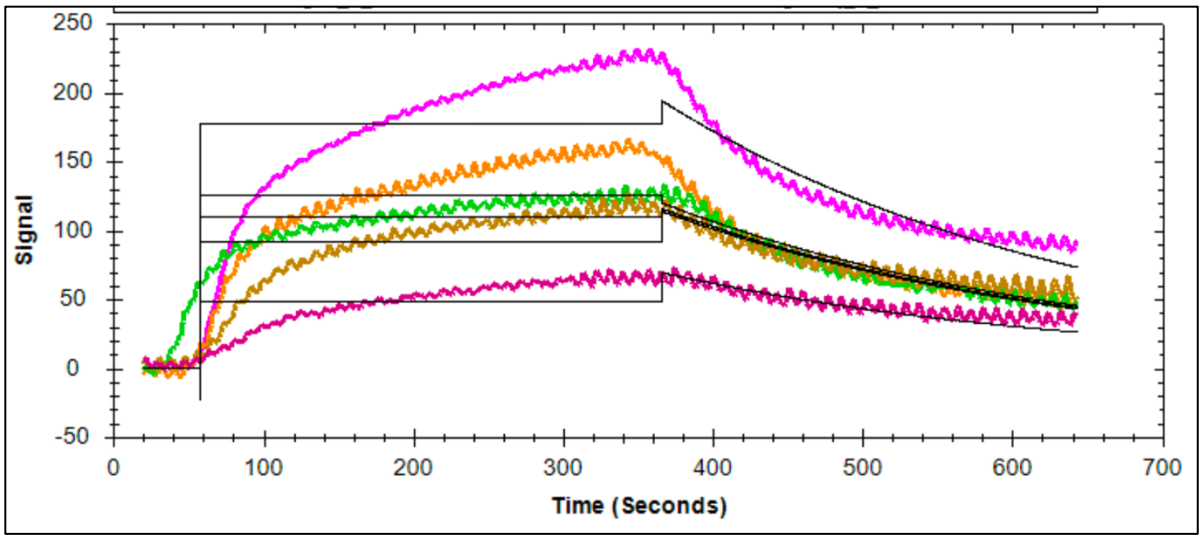


| Curve name | ka (1/(M*s)) | kd (1/s) | KD (M) |
|---|---|---|---|
| 14-GST 600ugml_0_6365.18S fitted | 1.00e5 (±6.86e7) | 3.52e-3 (±5.11e-5) | 3.52e-8 (±-5.13e-11) |
| 14-GST 300ugml_0_5620.33S fitted | 1.00e5 (±6.86e7) | 3.52e-3 (±5.11e-5) | 3.52e-8 (±-5.13e-11) |
| 14-GST 150 ugml valve ok_0_4426.66S fitted | 1.00e5 (±6.86e7) | 3.52e-3 (±5.11e-5) | 3.52e-8 (±-5.13e-11) |
| 14-GST 100ugml_0_3254.69S fitted | 1.00e5 (±6.86e7) | 3.52e-3 (±5.11e-5) | 3.52e-8 (±-5.13e-11) |
| 14-GST 50ugml inj_0_2599.72S fitted | 1.00e5 (±6.86e7) | 3.52e-3 (±5.11e-5) | 3.52e-8 (±-5.13e-11) |

***Figure 30.*** *Surface Plasmon Resonance measurements N-His-Lsd13 and tagless-Lsd14.*

Several crystallization experiments were performed using these two proteins, but no potential hit was found after more than 6 months; changing buffer or temperature didn't lead to any hit as well.

### 3.5.1. Crystallization experiments of N-His-Lsd13-ACP-long/tagless-Lsd14-KS-AT complex

The reason why we were not able to get the protein complex crystal could be related to the size of the complex, Lsd13 and Lsd14 are both homodimers with a molecular weight combined of almost 600 kDa. We started looking down for what domains we have to preserve in order to get a system that is smaller but give us the same information. For this we need the docking domains since these ones drive the inter-PKS communication, the docking domains are the one that select the up-stream partner synthase; as well we need to maintain the ACP domain from Lsd13 and the

KS-AT domain dimer for the chain transfer process that takes place when the substrate from the ACP is delivered to the KS domain of the up-stream PKS.

The system that we selected consisted in the ACP domain from Lsd13 including the docking domain at the C-term, named as Lsd13-ACP-long; and the KS-AT domains from Lsd14 named as Lsd14-KS-AT.

Crystallization experiments were done at 18 Celsius degrees using the NT8 robot with all the screens mentioned in the **Chapter 2.5**. After 8 days we got a potential initial hit in the Morpheus screen – condition well B9.

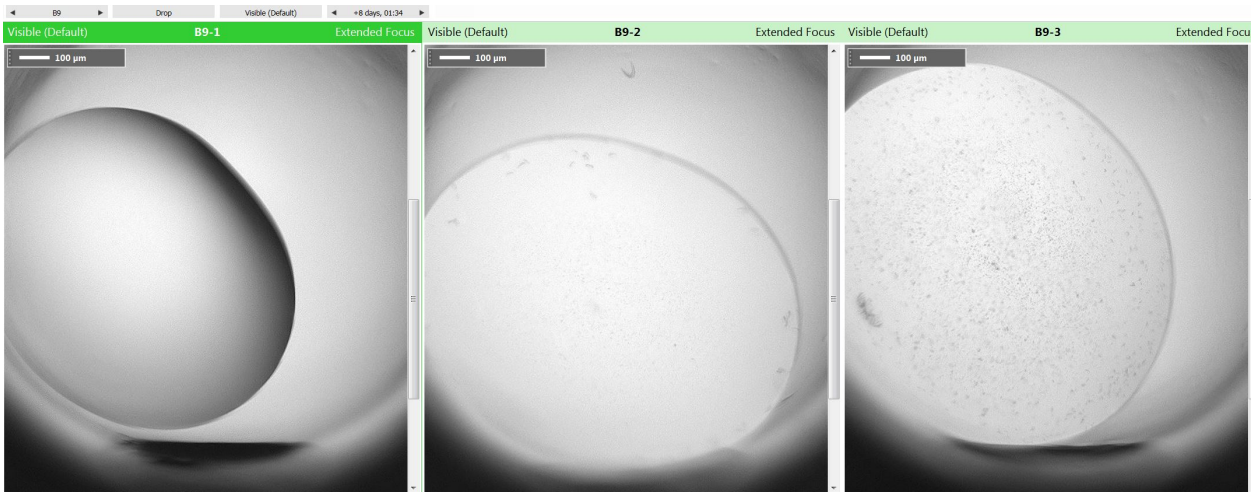


***Figure 31.*** *Initial hit protein complex Lsd13-ACP-long + Lsd14-KS-AT.*

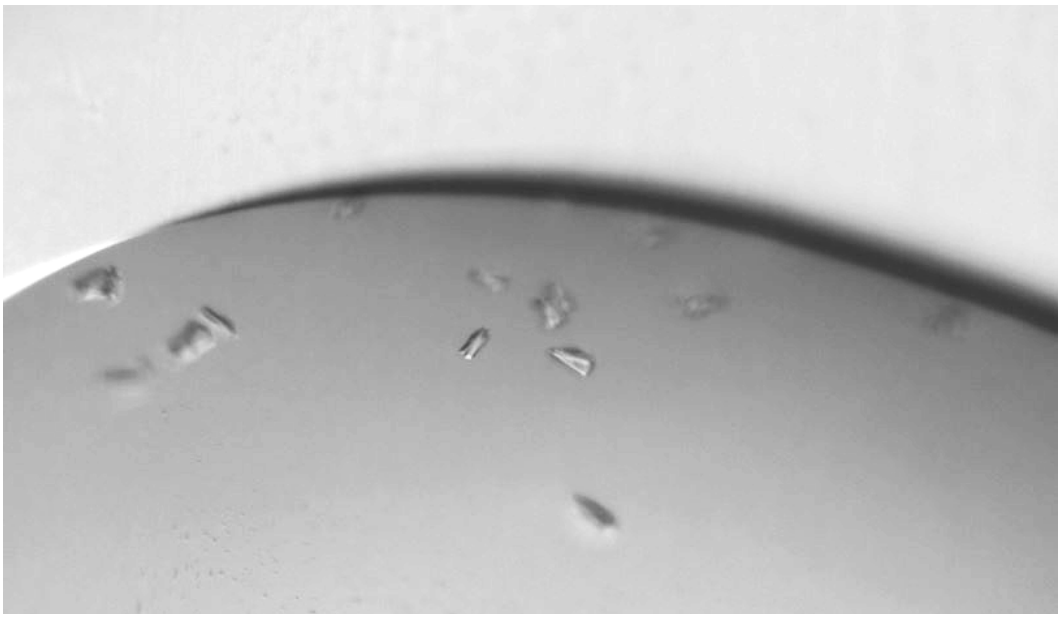

***Figure 32.*** *Initial hit zoom protein complex Lsd13-ACP-long + Lsd14-KS-AT.*

The initial protein crystal hit of Lsd13 is a needle-cluster type crystal, with tiny size covering the entire drop. Optimization of the crystal at the initial step was driven by the different components and concentration in the B9 condition from Morpheus screen.

**Morpheus B9:** precipitant mix - 10% PEG 20k, 20% MME 550; buffer – 0.1 M Bicine/ Tris pH = 8.5 and additive – Halide mix 0.03 M (NaI, NaBr and NaF).

Optimization experiments changing the precipitant mix from 5% to 40% in 5% increments and buffer pH from 6.0 to 11.0 in 0.5 increments were performed utilizing both sitting and hanging drop method with a drop size of 4 uL **(Figure #)**. Lastly seeding experiments we performed to increase the size of the crystal and obtain at least preliminary X-Ray diffraction data, but we were unable to reach a crystal size suitable for measurements.

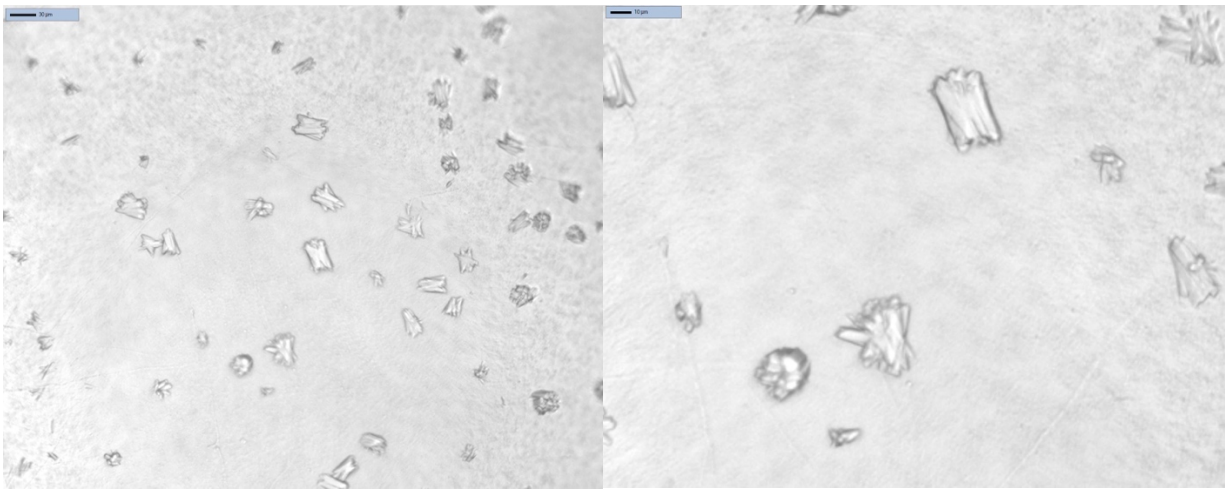

***Figure 33.*** *Optimized protein complex crystal Lsd13-ACP-long + Lsd14-KS-AT.*

In this case we didn't have access to a UV lamp to confirm that this crystal is protein crystal, even this will not give us information about the complex since Lsd13-ACP-long sequence only contains 2 tryptophan in the sequence, the UV signal is expected to be low.

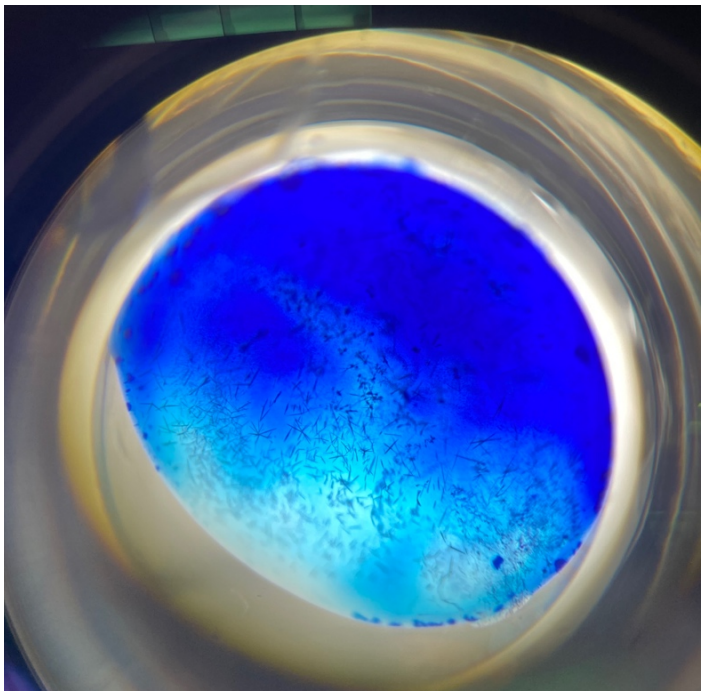

Izit dye is a dye used to differentiate protein crystals from salt crystals. In this case we used the Izit dye to confirm that is protein crystal and as a contrast agent to see if the crystals are break down easily with the crystallization tools. Now we are working with different additives screens, that possible will help with crystal grow or change the morphology.

***Figure 34.*** *Complex crystal Lsd13-ACP-long + Lsd14-KS-AT with Izit dye.*

## Conclusions and Future directions

Through this research, we achieved successful crystallization of a modular polyketide synthase Lsd13, consisting of the minimal domain composition KS-AT-ACP, as well as the fragmented complex Lsd13-ACP-Lsd14-KS-AT. The purification process of two polyketide synthases, Lsd13 and Lsd14, is detailed, along with the purification of a single domain, Lsd13-ACP, and the Lsd14-KS-AT fragment. Additional efforts should be made to enhance crystal quality and obtain a complete dataset for further analysis.

The crystal structure information of Lsd13 will give us a clear understanding of how polyketide synthase structure is determined and if PKS are a build-up system comparing with Lsd14 structure reported. Lsd13-ACP and Lsd14-KS-AT complex will provide structural insights on interaction of different modules in a modular polyketide synthesis pathway.

## References


Bagde, S. R., Mathews, I. I., Fromme, J. C., & Kim, C. Y. (2021). Modular polyketide synthase contains two reaction chambers that operate asynchronously. *Science*, *374*(6568). https://doi.org/10.1126/SCIENCE.ABI8532

Benvenuti, M., & Mangani, S. (2007). Crystallization of soluble proteins in vapor diffusion for x-ray crystallography. *Nature Protocols 2007 2:7*, *2*(7), 1633–1651. https://doi.org/10.1038/nprot.2007.198

Chayen, N. E., & Saridakis, E. (2008). Protein crystallization: from purified protein to diffraction-quality crystal. *Nature Methods 2008 5:2*, *5*(2), 147–153. https://doi.org/10.1038/nmeth.f.203

Darrow, J. J., Avorn, J., & Kesselheim, A. S. (2020). FDA Approval and Regulation of Pharmaceuticals, 1983-2018. *JAMA - Journal of the American Medical Association*, *323*(2), 164–176. https://doi.org/10.1001/jama.2019.20288

Dauter, Z. (2017). Collection of X-ray diffraction data from macromolecular crystals. *Methods in Molecular Biology*, *1607*, 165–184. https://doi.org/10.1007/978-1-4939-7000-1_7/COVER

Duax, W. L., Griffin, J. F., Langs, D. A., Smith, G. D., Grochulski, P., Pletnev, V., & Ivanov, V. (1996). Molecular structure and mechanisms of action of cyclic and linear ion transport antibiotics. *Biopolymers*, *40*(1), 141–155. https://doi.org/10.1002/(sici)1097-0282(1996)40:1<141::aid-bip6>3.3.co;2-b

Dzikamunhenga, R. S., & Griffith, R. (2012). *Safety evaluation of lasalocid use in farm-reared pheasants*.

Gawas, U. B., Mandrekar, V. K., & Majik, M. S. (2019). Structural analysis of proteins using X-ray diffraction technique. In *Advances in Biological Science Research: A Practical Approach*. Elsevier Inc. https://doi.org/10.1016/B978-0-12-817497-5.00005-7

Gershell, L. J., & Atkins, J. H. (2003). A brief history of novel drug discovery technologies. *Nature Reviews Drug Discovery*, *2*(4), 321–327. https://doi.org/10.1038/nrd1064

Katz, L. (1997). Manipulation of modular polyketide synthases. *Chemical Reviews*, *97*(7), 2557–2575. https://doi.org/10.1021/cr960025+

Kennedy, J. P., Williams, L., Bridges, T. M., Daniels, R. N., Weaver, D., & Lindsley, C. W. (2008). Application of combinatorial chemistry science on modern drug discovery. *Journal of Combinatorial Chemistry*, *10*(3), 345–354. https://doi.org/10.1021/cc700187t

Kurt Yilmaz, N., & Schiffer, C. A. (2021). Introduction: Drug Resistance. *Chemical Reviews*, *121*(6), 3235. https://doi.org/10.1021/ACS.CHEMREV.1C00118

Lam, K. S. (2007). New aspects of natural products in drug discovery. *Trends in Microbiology*, *15*(6), 279–289. https://doi.org/10.1016/j.tim.2007.04.001

Li, Y., Xu, W., & Tang, Y. (2010). Classification, prediction, and verification of the regioselectivity of fungal polyketide synthase product template domains. *Journal of Biological Chemistry*, *285*(30), 22764–22773. https://doi.org/10.1074/jbc.M110.128504

Liu, R., Li, X., & Lam, K. S. (2017). Combinatorial chemistry in drug discovery. *Current Opinion in Chemical Biology*, *38*, 117–126. https://doi.org/10.1016/j.cbpa.2017.03.017

McPherson, A., & Gavira, J. A. (2014). Introduction to protein crystallization. *Acta Crystallographica. Section F, Structural Biology Communications*, *70*(Pt 1), 2. https://doi.org/10.1107/S2053230X13033141

Migita, A., Watanabe, M., Hirose, Y., Watanabe, K., Tokiwano, T., Kinashi, H., & Oikawa, H. (2009). Identification of a gene cluster of polyether antibiotic lasalocid from Streptomyces lasaliensis. *Bioscience, Biotechnology and Biochemistry*, *73*(1), 169–176. https://doi.org/10.1271/bbb.80631

Moretto, L., Heylen, R., Holroyd, N., Vance, S., & Broadhurst, R. W. (2019). Modular type I polyketide synthase acyl carrier protein domains share a common N-terminally extended fold. *Scientific Reports 2019 9:1*, *9*(1), 1–16. https://doi.org/10.1038/s41598-019-38747-9

Nakata, T., Schmid, G., Vranesic, B., Okigawa, M., Smith-Palmer, T., & Kishi, Y. (1978). A Total Synthesis of Lasalocid A. *Journal of the American Chemical Society*, *100*(9), 2933–2935. https://doi.org/10.1021/JA00477A081/ASSET/JA00477A081.FP.PNG_V03

Parker, M. W. (2003). Protein Structure from X-Ray Diffraction. *Journal of Biological Physics*, *29*(4), 341–362. https://doi.org/10.1023/A:1027310719146

Ridley, C. P., Ho, Y. L., & Khosla, C. (2008). Evolution of polyketide synthases in bacteria. *Proceedings of the National Academy of Sciences of the United States of America*, *105*(12), 4595–4600. https://doi.org/10.1073/pnas.0710107105

Risdian, C., Mozef, T., & Wink, J. (2019). Biosynthesis of polyketides in Streptomyces. *Microorganisms*, *7*(5), 1–18. https://doi.org/10.3390/microorganisms7050124

Robinson, J. A. (1991). Polyketide synthase complexes: their structure and function in antibiotic biosynthesis. *Philosophical Transactions of the Royal Society of London. Series B, Biological Sciences*, *332*(1263), 107–114. https://doi.org/10.1098/rstb.1991.0038

Shen, B. (2003). Polyketide biosynthesis beyond the type I, II and III polyketide synthase paradigms. *Current Opinion in Chemical Biology*, *7*(2), 285–295. https://doi.org/10.1016/S1367-5931(03)00020-6

Taber, D. (2011). Stereoselective C-O Ring Construction: The Oguri-Oikawa Synthesis of Lasalocid A. *Organic Synthesis*. https://doi.org/10.1093/OSO/9780199764549.003.0047

Tang, Y., Kim, C. Y., Mathews, I. I., Cane, D. E., & Khosla, C. (2006). The 2.7-Å crystal structure of a 194-kDa homodimeric fragment of the 6-deoxyerythronolide B synthase. *Proceedings of the National Academy of Sciences of the United States of America*, *103*(30), 11124–11129. https://doi.org/10.1073/PNAS.0601924103

Wang, B., Guo, F., Huang, C., & Zhao, H. (2020). Unraveling the iterative type I polyketide synthases hidden in Streptomyces. *Proceedings of the National Academy of Sciences of the United States of America*, *117*(15), 8449–8454. https://doi.org/10.1073/pnas.1917664117

Wang, L., Yuan, M., & Zheng, J. (2019). Crystal structure of the condensation domain from lovastatin polyketide synthase. *Synthetic and Systems Biotechnology*, *4*(1), 10–15. https://doi.org/10.1016/J.SYNBIO.2018.11.003

Wang, W., Arshad, M. I., Khurshid, M., Rasool, M. H., Nisar, M. A., Aslam, M. A., & Qamar, M. U. (2018). Antibiotic resistance : a rundown of a global crisis. *Infection and Drug Resistance*, 1645–1658.

Weissman, K. J. (2009). Chapter 1 Introduction to Polyketide Biosynthesis. *Methods in Enzymology*, *459*(B), 3–16. https://doi.org/10.1016/S0076-6879(09)04601-1

Zhang, M. M., Wong, F. T., Wang, Y., Luo, S., Lim, Y. H., Heng, E., Yeo, W. L., Cobb, R. E., Enghiad, B., Ang, E. L., & Zhao, H. (2017). CRISPR-Cas9 strategy for activation of silent Streptomyces biosynthetic gene clusters. *Nature Chemical Biology*, *13*(6), 607–609. https://doi.org/10.1038/nchembio.2341

## Curriculum Vita

B.S. Dayan Viera is a PhD candidate in the Department of Chemistry and Biochemistry at The University of Texas at El Paso (UTEP), under the guidance of Dr. Chu-Young Kim. He holds a B.S. degree in Chemistry from The University of Havana, Cuba, where he was advised by Dr. Daniel Garcia Rivera. With a GPA of 3.95/4.00 in his doctoral studies and 4.40/5.00 in his undergraduate studies, Dayan has excelled academically. He has served as a teaching assistant for General Chemistry, Introduction to Organic and Biochemistry and Organic Chemistry courses at UTEP since 2019. Prior to that, he worked as a researcher at the Vaccine Finlay Institute in Havana, Cuba, from 2018 to 2019. Dayan has presented his research findings at various conferences and symposiums, including the Young Researcher event at the Vaccine Finlay Institute, where he discussed the synthesis of Capsular polysaccharides conjugates of Streptococcus pneumoniae to α-Galactosylceramide analogues. He also presented his work at QUIMI-CUBA, the Scientific day at Vaccine Finlay Institute, and the Ernest L. Eliel Symposium, among others. Dayan can be contacted via email at **dviera@miners.utep.edu** and his LinkedIn profile can be found at linkedin.com/in/dayanviera.